Given the role of HDACs in oncogenesis, the use of small compounds that inhibit HDAC activity, collectively referred to as HDAC inhibitors, is expected to become a novel strategy for the treatment of cancer called 'transcription therapy' (Somech *et al.*, 2004). HDAC inhibitors are able to restore the expression of genes that are aberrantly suppressed in cancer cells, which may result in cell cycle arrest, differentiation, and apoptosis (Kim *et al.*, 2003). Because the principle of action differs from that of other anticancer drugs, HDAC inhibitors may be effective for malignancies that are otherwise resistant to conventional chemotherapy. Indeed, HDAC inhibitors have been shown to exert cytotoxic effects on various tumor cell lines and primary cancer cells *in vitro* (Hoshikawa *et al.*, 1994). Furthermore, Zhu *et al.* (2004) reported that HDAC inhibitors were capable of reducing tumor formation on intestinal tracts of mice bearing mutations in the adenomatous polyposis coli (APC) tumor suppressor gene. Currently, phase I and II clinical trials are ongoing for four different types of HDAC inhibitors, namely sodium phenylbutyrate, FK228 (a bacterial depsipeptide, formerly FR901228), suberoylanilide hydroxamic acid (SAHA), and MS-275, in hematologic malignancies and various solid tumors (Gore *et al.*, 2002; Sandor *et al.*, 2002).

FK228 is one of the most promising HDAC inhibitors for the treatment of malignant melanoma because of its potent antitumor activity. This drug was isolated from *Chromobacterium violaceum* No. 968 as a compound that reversed the malignant phenotypes of H-ras-transformed fibroblasts by blocking the $p21^{ras}$-mediated signal transduction pathways (Ueda *et al.*, 1994). In independent studies, FK228 was identified as a microbial metabolite that induces transcriptional activation of the SV40 promoter via inhibition of intracellular HDAC activities (Nakajima *et al.*, 1998; Furumai *et al.*, 2002). FK228 was reported to inhibit proliferation and induce apoptosis in primary and metastatic uveal melanoma cell lines *in vitro* (Klisovic *et al.*, 2003), and exhibited therapeutic effects on a diverse range of malignancies, including melanoma, in phase I and II clinical trials (Gore *et al.*, 2002; Sandor *et al.*, 2002). However, the safe and effective clinical application of this agent will require clarification of the molecular basis of its cytotoxic activity. In the present study, we investigated the cytotoxic effect of FK228 on malignant melanoma and its mechanism of action using six melanoma cell lines. We have found that (1) FK228 is more effective against malignant melanoma than other commonly used anticancer drugs, (2) the cytotoxic effects of FK228 are at least in part mediated by the upregulation of Rap1, a small GTP-binding protein of the Ras family, and (3) Rap1 is an intrinsic regulator of the Ras–Raf–MAP kinase signaling pathway in melanoma cells.

Results

FK228 is more effective for malignant melanoma than other commonly used anticancer drugs

We first evaluated the therapeutic efficacy of FK228 against malignant melanoma. For this purpose, we cultured the human melanoma cell line MM-LH with various concentrations of FK228 and other drugs commonly used for the treatment of melanoma, and determined the level of 5-bromo-2′-deoxyuridine (BrdU) incorporation after 48 h. As shown in Figure 1a, FK228 effectively inhibited the growth of MM-LH in a dose-dependent manner; BrdU incorporation decreased to less than 50% of that of the untreated control with 100 nM of the drug and to approximately 10% at a dose of 1 μM, which corresponds to the mean maximum plasma concentration ($C_{max.}$) determined in phase I clinical trials (Sandor *et al.*, 2002). In contrast, the other three drugs (adriamycin, vincristine, and interferon-β) failed to induce a decrease in BrdU incorporation at $C_{max.}$ (Figure 1a). The difference in the efficacy between FK228 and other drugs was statistically significant ($P<0.001$).

Next, we examined the cytotoxic effects of FK228 on normal human melanocytes. As shown in Figure 1b, FK228 was found to be less toxic to normal human epidermal melanocytes (NHEM) grown in the presence of melanocyte-growth medium than to three other melanoma cell lines MM-AN, MM-BP, and RPM-MC ($P<0.001$).

We further confirmed the antimelanoma effects of the drug *in vivo* using an animal model system. SCID mice carrying subcutaneous MM-LH xenografts were treated with intraperitoneal injection of FK228. As shown in Figure 1c, FK228 significantly retarded the growth of the xenografts compared with control (phosphate-buffered saline (PBS) alone) ($P=0.016$ at day 20) without obvious side effects. Taken together, these results strongly encourage the clinical application of FK228 for malignant melanoma.

DNA chip analysis has revealed candidate FK228 effector genes

Because the principal mechanism of action of HDAC inhibitors is the modulation of transcription, it is reasonable to screen for changes in gene expression as an initial step in exploring the mechanisms of the cytotoxic effects of FK228. To determine the optimal conditions for gene expression analysis, we first determined the time course of the effects of FK228 using the MM-LH cell line. Cell cycle analysis was serially performed with MM-LH cells cultured in the absence or presence of FK228 at a concentration of 100 nM, approximately the IC_{50} of this drug. FK228 induced both cell cycle arrest at the G1 phase and apoptosis, as judged by the appearance of the sub-G1 fraction (Figure 1d, upper panel), DNA fragmentation in the nuclei (Figure 1d, lower panel), and annexin V-positive cells (data not shown), after 24 h of culture. The time course of the response to the drug was almost identical to that of other melanoma cell lines (data not shown).

According to this result, we decided to perform a DNA chip analysis using RNA samples isolated at 6 h of culture, a time point at which the changes on the DNA histograms were minimal. The results of the analysis are summarized in Table 1: 20 genes showed more than a

fivefold increase in mRNA expression after FK228 treatment among 3893 human cancer-related and cytokine genes screened. The same analysis was performed using normal melanocytes in order to determine the subset of genes specifically upregulated in melanoma cells. We provisionally defined FK228 effector genes as

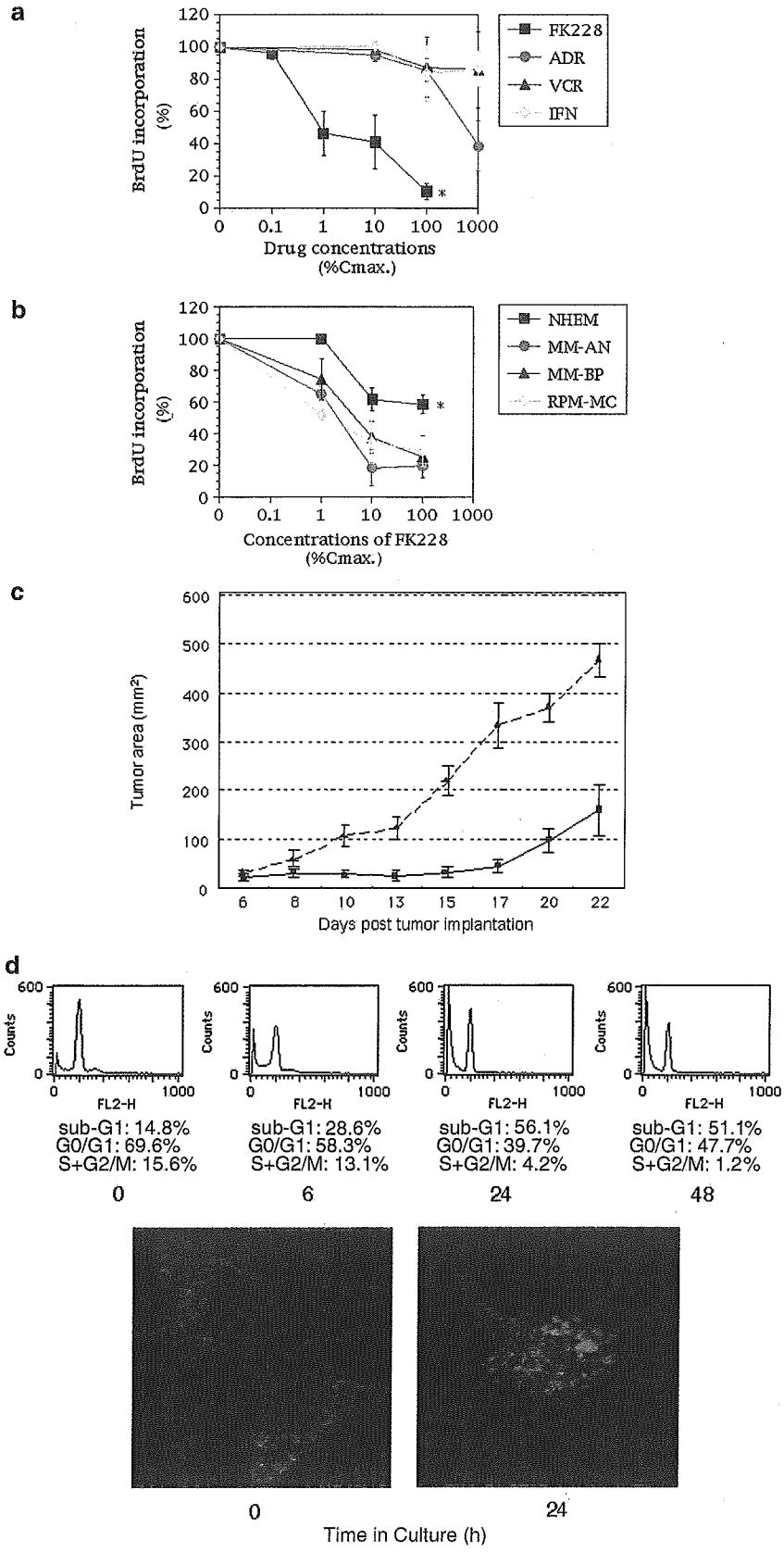

follows: genes upregulated more than fivefold in melanoma cells and less than twofold in normal melanocytes. Among 20 FK228-induced genes, seven genes fulfilled the criteria for FK228 effector genes: Silver-like (gp100/pMel17), TNF-α-induced protein 6, Rap1A, ADP-ribosylation factor 4, FLJ23028 (c-mer homolog), Coiled-coil forming protein 1, and TFIIB (Table 1). We chose Rap1 for further investigation of its involvement in the antimelanoma effects of FK228, because Rap1, a small GTP-binding protein of the Ras family, was originally isolated as Krev-1 by virtue of its ability to revert the malignant phenotype of activated Ras-transformed fibroblasts back to normal (Kitayama *et al*., 1989), which is identical to the approach used for the initial discovery of FK228.

FK228 increases the expression of Rap1 and suppresses the activity of other components of the Ras–MAP kinase signaling pathway in melanoma cells

To confirm the upregulation of Rap1 by FK228, we carried out Northern blotting using MM-LH and RPM-MC melanoma cell lines. Consistent with the results of the DNA chip analysis, the abundance of the Rap1 (Rap1A) transcript increased more than fivefold in FK228-treated cells, whereas no change was observed in untreated cells (Figure 2a, and data not shown). Importantly, the level of Rap1A mRNA remained below the detection limit in NHEM, even after treatment with FK228. We simultaneously examined the expression of Rap1B, a close relative of Rap1A/Krev-1 with a different chromosomal location (Bokoch,

Table 1 Genes whose expression was increased more than fivefold following FK228 treatment of melanoma cells[a]

Gene name[b]	*Accession number*	*Fold increase*[c]	*Increase in normal melanocytes*[d]
Interleukin-8	NM_000584	25.40 (94/3.7)	5.00 (74/14.8)
Fatty acid-binding protein 4	NM_001445	22.84 (1695/74.2)	122.54 (13968/114)
Silver-like	NM_006928	15.12 (270/17.85)	0.80 (48789/60986)
TNF-α-induced protein 6	NM_007115	12.55 (1066/84.9)	Not detected
Rap1A	BC034049	8.81 (690/78.3)	1.20 (32/26.7)
c-*fos*	NM_005252	8.21 (752/91.6)	5.71 (353/61.8)
SBB126	AK056390	7.49 (752/100.4)	2.76 (186/67.4)
ADP-ribosylation factor 4	NM_001661	7.23 (276/38.2)	1.58 (186/118)
FLJ23028	AK026681	6.23 (87/13.96)	0.88 (2/2.3)
Lipin1	D80010	5.76 (612/106.3)	2.23 (281/126)
FLJ22548	NM_022456	5.70 (439/77)	3.99 (289/72.4)
KIAA0870	AB020677	5.39 (123/22.8)	54.07 (260/4.80)
Coiled-coil forming protein 1	NM_014781	5.31 (1833/345.2)	1.96 (345/176)
KIAA0080	D38522	5.30 (1099/207.4)	9.95 (1359/136.6)
CDABP0105	AY007156	5.29 (270/51)	8.86 (207/23.4)
Nerve growth factor receptor	NM_002507	5.22 (152/29.1)	4.79 (150/31.3)
TFIIB	M76766	5.18 (799/154.2)	1.74 (603/346.6)
FEN1/Elo2	NM_022726	5.15 (164/31.8)	3.15 (73/23.2)
MHC class II peptide-related sequence A	NM_000247	5.12 (550/107.4)	4.62 (947/205)
Ephrin-B2	NM_004093	5.10 (44/8.63)	2.35 (76/32.3)

[a]Poly(A) RNAs were isolated from MM-LH cells treated with 100 nM FK228 for 6 h and from the untreated control, labeled with Cy5 and Cy3, respectively, and were hybridized to IntelliGene II human CHIP version 1.0 (Takara), which contains cDNA fragments of 3893 human cancer-related and cytokine genes. Precise information about this array is available at the company's website (http://www.takara.com). [b]FK228 effector genes are highlighted in bold (see text for definition). [c]Normalized expression values are shown in parentheses (treated/untreated). [d]The same experiments were carried out using normal human epidermal melanocytes.

Figure 1 Sensitivity of melanoma cells and normal melanocytes to FK228. (**a**) MM-LH cells were exposed to various concentrations of FK228, adriamycin (ADR), vincristine (VCR), and interferon-β (IFN-β) for 48 h, and cell growth was monitored by BrdU incorporation. Drug concentrations are expressed as the percentage of the mean maximum plasma concentration at the maximum tolerated dose (%$C_{max.}$). The $C_{max.}$ is 1 μM, 1 μg/ml, 100 nM, and 1000 U/ml for FK228, ADR, VCR, and IFN, respectively. BrdU incorporation is shown as the percentage of the value obtained with untreated cells. The results are the means ± s.d. (bar) of three independent experiments. Statistical analysis was performed using the Student's *t*-test to compare the data from cells treated with FK228 and other drugs (an asterisk denotes $P<0.001$). (**b**) The same experiments were performed with NHEM and three different melanoma cell lines. Statistical analysis was carried out using the Student's *t*-test for comparative analysis of the data from NHEM and other cell lines (an asterisk denotes $P<0.001$). (**c**) MM-LH cells (1×10^7 cells/mouse) were injected subcutaneously into SCID mice. After tumors were palpable, animals were treated with either FK228 (0.5 mg/kg, intraperitoneally, every other day) or PBS. Serial measurement of tumor sizes in FK228- and PBS-treated mice was made. Slide line: FK228 treatment; dashed line: PBS treatment. Data represent the means ± s.d. ($n=5$). Statistical analysis was carried out using the Mann–Whitney U test ($P=0.016$ at day 20). (**d**) MM-LH cells were seeded at 1×10^5 cells/ml and cultured in the presence of 100 nM FK228 for 48 h. Cells were harvested at the indicated time points, and subjected to cell cycle analysis (upper panel) and a TUNEL assay (lower panel). The size of the sub-G1, G0/G1, and S + G2/M fractions was calculated using the ModFitLT 2.0 program, and the results are shown below each DNA histogram. The data shown are representative of three independent experiments.

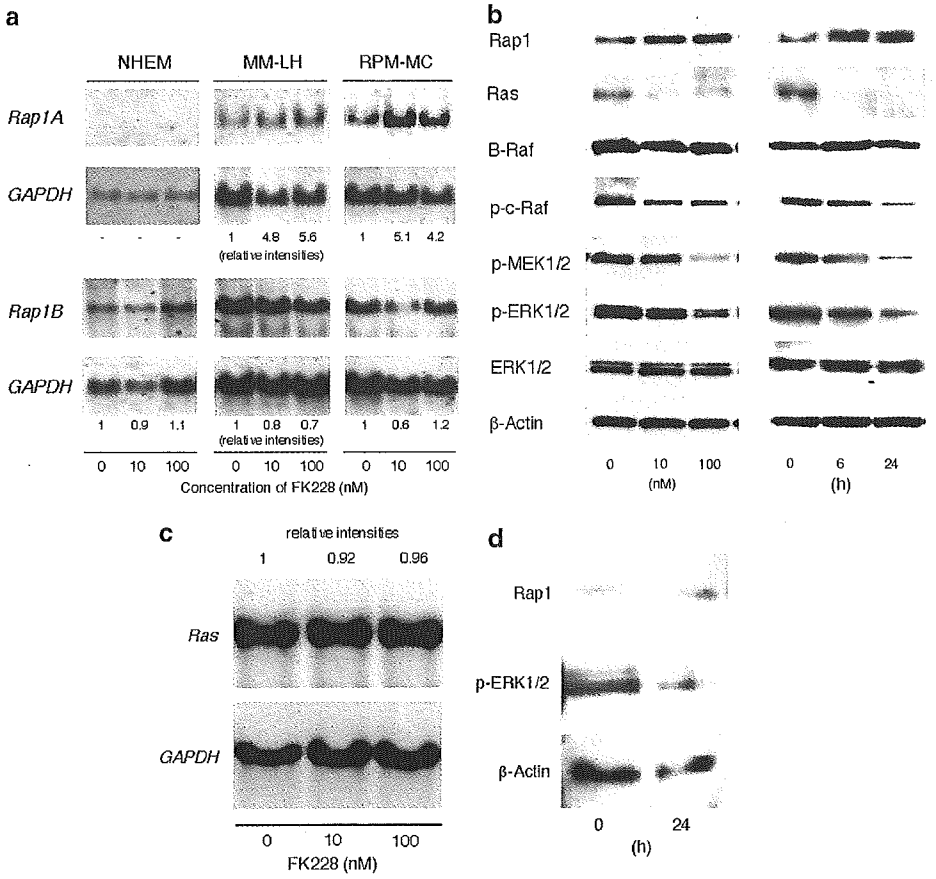

Figure 2 Expression of Rap1 and the components of the Ras–MAP kinase signaling pathway in FK228-treated melanoma cells and normal melanocytes. (**a**) Total cellular RNA was isolated from normal melanocytes (NHEM), and MM-LH and RPM-MC cell lines cultured with the indicated concentrations of FK 228 for 24 h, and was subjected to Northern blot analysis for Rap1A and Rap1B mRNA expression. The membrane filters were rehybridized with glyceroaldehyde-3-phosphate dehydrogenase (GAPDH) cDNA to serve as a loading control. The relative intensities of the signals were calculated as the fold increase from the value obtained in untreated cells (FK228 0 nM) after being normalized to the signal intensities of the corresponding GAPDH transcripts. (**b**) Whole-cell lysates were prepared from MM-LH cells cultured with various concentrations of FK228 for 24 h or with 100 nM FK228 for the indicated periods of time. The expression of Rap1 and the indicated components of the Ras–Raf–ERK signaling pathway was examined by immunoblotting using specific antibodies (p- indicates phosphorylated species). The membrane filters were reprobed with β-actin antibody in order to verify the equal loading of samples. (**c**) Ras mRNA expression was examined by Northern blotting in FK228-treated MM-LH cells. Relative signal intensities are shown on top. (**d**) Normal human melanocytes were cultured in the growth medium in the presence of 100 nM FK228 for 24 h, and subjected to immunoblotting for Rap1 and phosphorylated ERK1/2.

1993; Noda, 1993), and found that Rap1B mRNA expression was constitutive in both normal and malignant melanocytes, and was not affected by FK228.

It has been reported that Rap1A/Krev-1 inhibits Ras-mediated ERK activation via competitive interference with c-Raf kinase as an antagonist of Ras (Kitayama *et al*., 1989; Cook *et al*., 1993; Hu *et al*., 1997). We therefore examined the expression and activation status of the components of the Ras–Raf–MEK1/2–ERK1/2 pathway in FK228-treated melanoma cells by immunoblotting using activation-state antibodies. First, we confirmed the upregulation of Rap1 at the protein level. In accord with the observed increase in mRNA expression, the amount of Rap1 protein was increased by FK228 in both a dose- and a time-dependent manner (Figure 2b). The upregulation of Rap1 was accompanied by a decrease in the phosphorylated/activated forms of c-Raf, MEK1/2, and ERK1/2, whereas the total amounts of these proteins and B-Raf did not change (Figure 2b, and data not shown). In addition, FK228 decreased the expression of $p21^{Ras}$ in melanoma cells. The down-regulation of Ras was considered to be translational or post-translational, because FK228 did not reduce the abundance of the Ras transcript (Figure 2c). Other members of MAP kinase pathways, such as p38 MAP kinase and SAPK/JNK, were not activated in the melanoma cell lines used in our study (data not shown).

In addition, we performed a similar analysis using normal melanocytes, which are relatively resistant to the drug. As shown in Figure 2d, Rap1 protein was only marginally increased in FK228-treated normal melanocytes, which is compatible with the results of Northern blotting. FK228 induced a decrease in the level of phosphorylated ERK1/2 in normal melanocytes less than that in melanoma cells; the reduction rates after normalization to β-actin levels are 56.0% in normal melanocytes (Figure 2d) and 83.4% in MM-LH cells (Figure 2b) at 24 h of culture with FK228. This

reduction is well correlated with the decrease in BrdU incorporation, suggesting that FK228-mediated growth suppression is closely associated with the modulation of Rap1/Ras–ERK1/2 signaling components.

Cytotoxic effects of FK228 are at least in part mediated by the upregulation of Rap1 in melanoma cells

To determine whether the inhibition of Ras–Raf–ERK1/2 signaling was a direct effect of FK228 or was mediated by Rap1, we examined the effects of exogenous Rap1 overexpression on cell viability and the activation status of Ras–MAP kinase cascade components. Forced expression of both wild-type and activated Rap1 (Kitayama *et al.*, 1990) resulted in an increase in the size of the sub-G1 fraction (Figure 3a) and a decrease in phosphorylated/activated ERK1/2 (Figure 3b) in MM-LH cells, suggesting that the upregulation of Rap1 *per se* can confer a suppression of MAP kinase activity, thereby leading melanoma cells to apoptosis. Unexpectedly, Ras expression was suppressed by exogenous Rap1 (Figure 3b), raising the possibility that Rap1 also mediates the downregulation of Ras in FK228-treated melanoma cells. However, the involvement of other factors, such as other 'FK228 effector genes', is highly likely, because the magnitude of apoptosis observed here is lower than that of FK 228-treated cells: approximately 40% in Rap1-overexpressing cells (Figure 3a) vs more than 50% in FK228-treated cells (Figure 1d).

To further corroborate the role of Rap1 in the cytotoxic activity of FK228, we attempted to abrogate the drug effect by interfering with the upregulation of Rap1 with small interfering RNA (siRNA). As shown in Figure 4a and b, siRNA against Rap1, but not control siRNA, effectively blocked the FK228-induced increase in Rap1. In the presence of Rap1 siRNA, FK228 was unable to induce either apoptosis (Table 2) or the inactivation of ERK1/2 (Figure 4c) in MM-LH cells. In addition, the downregulation of Ras was also canceled by Rap1 siRNA (data not shown), suggesting the causal relationship between Rap1 induction and Ras suppression. Taken together, these results indicate that the cytotoxicity of FK228 is at least in part mediated by the upregulation of Rap1.

Rap1 is an endogenous regulator of the Ras–MAP kinase signaling pathway in melanoma cells

Recent investigations have revealed that the abnormalities among Raf family members, such as activating mutations in the BRAF gene and c-Raf hyperactivity, are observed in most patients with malignant melanoma (Hubbard, 2004; Wan *et al.*, 2004). We therefore examined the presence of these abnormalities and their respective relationships to Rap1 in melanoma cell lines. T1796A substitution of the BRAF gene, which results in a V599E amino-acid change, was detected in two of the six cell lines used in this study (MM-Ac and MM-RU), whereas no mutations were detected in other portions of exon 15, nor anywhere in exon 11 (data not shown). The hyperactivity of c-Raf kinase, as judged by increased autophosphorylation, was observed in the MM-LH cell line (data not shown). As a result of these abnormalities, ERK1/2 was constitutively activated in MM-Ac, MM-RU, and MM-LH cell lines (Figure 5a). Despite the absence of known mutations, ERK1/2 was also hyperphosphorylated in three other cell lines, as compared to that in normal melanocytes, suggesting that the deregulation of the Ras–MAP kinase cascade is universally

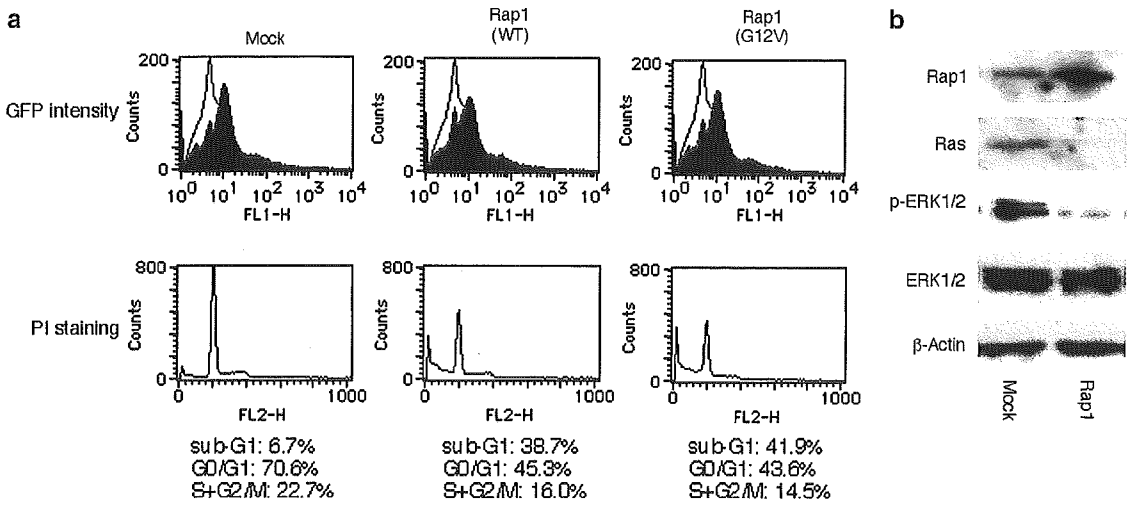

Figure 3 Effects of Rap1 overexpression on cell viability and ERK1/2 phosphorylation. (**a**) MM-LH cells were transfected with 2 μg of either an empty pcDNA 3.1 vector (Mock), a pcDNA 3.1 vector containing wild-type Rap1A/Krev-1 (WT), or a G12V active mutant (G12 V) and 1 μg of pIRES2-EGFP vector using LipofectAMINE 2000. After 48 h, the cells were harvested and subjected to flow cytometric analysis for GFP intensity and cell cycle profile using propidium iodide (PI) staining. In the upper panel, the filled and empty lines indicate transfected cells and untreated controls, respectively. The calculated sizes of the sub-G1, G0/G1, and S + G2/M fractions are shown below each DNA histogram. (**b**) Whole-cell lysates were simultaneously prepared and subjected to immunoblot analysis for Rap1, Ras, phosphorylated ERK1/2, total ERK1/2, and β-actin expression.

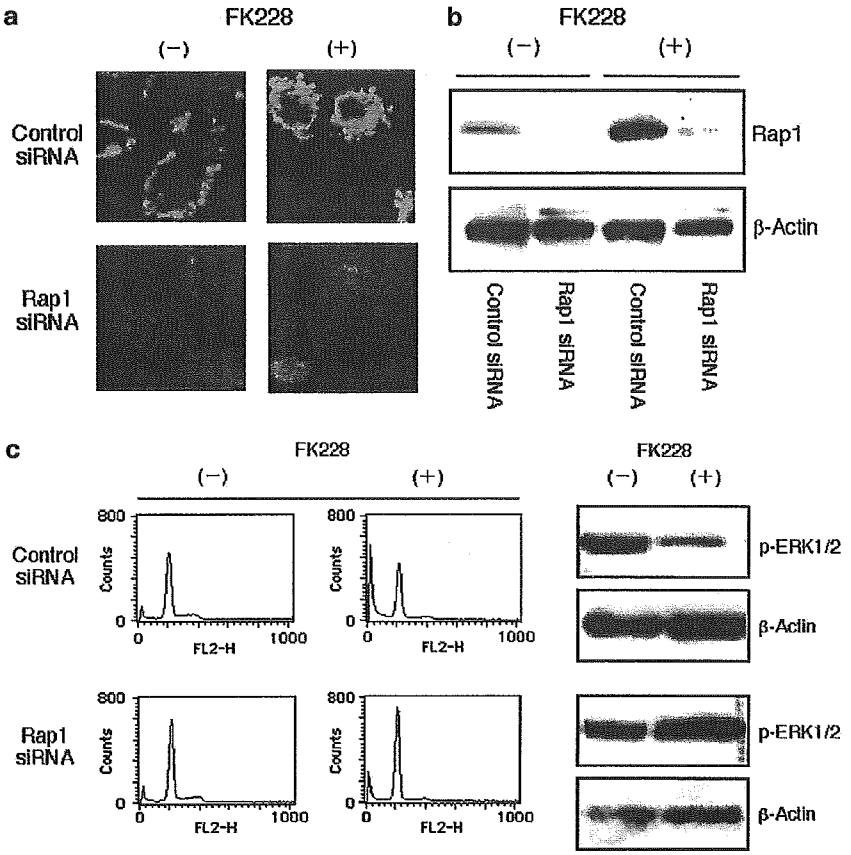

Figure 4 Effects of siRNA against Rap1 on cell viability and ERK1/2 phosphorylation. MM-LH cells were transfected with 3 μg of an equimolar mixture of either a pcPURU6βicassette vector containing TA0024-01, TA0024-02, and TA0024-03 (siRNA) or their corresponding scrambled sequences (Control). After 48 h, the cells were split into equal amounts and were respectively placed into two dishes, and FK228 was added into one of these dishes at a final concentration of 100 nM (+). After an additional 24 h of culture, the cells were stained with anti-Rap1 antibody in preparation for confocal microscopy (**a**), or subjected to immunoblotting for Rap1 expression (**b**) and ERK1/2 phosphorylation (**c**, right panel) and cell cycle analysis (**c**, left panel). β-Actin expression is shown as a loading control. The quantified results of cell cycle analysis are shown in Table 2.

Table 2 Cell cycle profile of siRNA-treated MM-LH cells

siRNA	*Cell cycle profile*[a]	*FK228*	
		(−)	*(+)*
Control siRNA	Sub-G1	13.9%	32.3%
	G0/G1	76.9%	54.8%
	S+G2/M	9.2%	12.9%
Rap1 siRNA	Sub-G1	13.7%	9.3%
	G0/G1	69.2%	73.3%
	S+G2/M	17.1%	17.4%

[a]The data shown in Figure 4c were quantified using the ModFit LT 2.0 program (Verity Software, Topsham, ME, USA).

present in melanoma cells (Figure 5a). Interestingly, the cell lines with an activating BRAF mutation were revealed to overexpress Rap1, whereas the Rap1 levels were relatively low in the other cell lines (Figure 5a). An abundance of Rap1 was negatively correlated with a sensitivity to FK228; the cell lines showing BRAF mutation/Rap1 overexpression were relatively resistant to the apoptosis-inducing effects of the drug (Figure 5b and Table 3 for quantification). This may be due to the inability of FK228 to further increase the abundance of Rap1 in these cells (Figure 5c). These results again provide support for the putative role of Rap1 as a mediator of the effects of FK228.

Finally, we attempted to elucidate the significance of Rap1 overexpression in melanoma cells with a BRAF mutation. Immunoprecipitation/immunoblot analysis revealed that Rap1 formed a complex with B-Raf in MM-RU cells, although this association was also observed in MM-LH cells lacking a BRAF mutation (Figure 6a). The complex formation was also visible on confocal microscopy in both cell lines (Figure 6b, yellow signals are indicative of colocalization). To investigate the function of endogenous Rap1 in melanoma cells, we targeted Rap1 by using siRNA. As shown in Figure 6c, the siRNA-mediated decay of Rap1 resulted in a decrease in the occurrence of spontaneous apoptosis and an increase in the number of cells in the S phase of the cell cycle among MM-RU cells. These results suggest that Rap1 acts as an endogenous suppressor of the hyperactivity of mutated B-Raf in some melanoma cells, and the presence of a feedback link between B-Raf and Rap1.

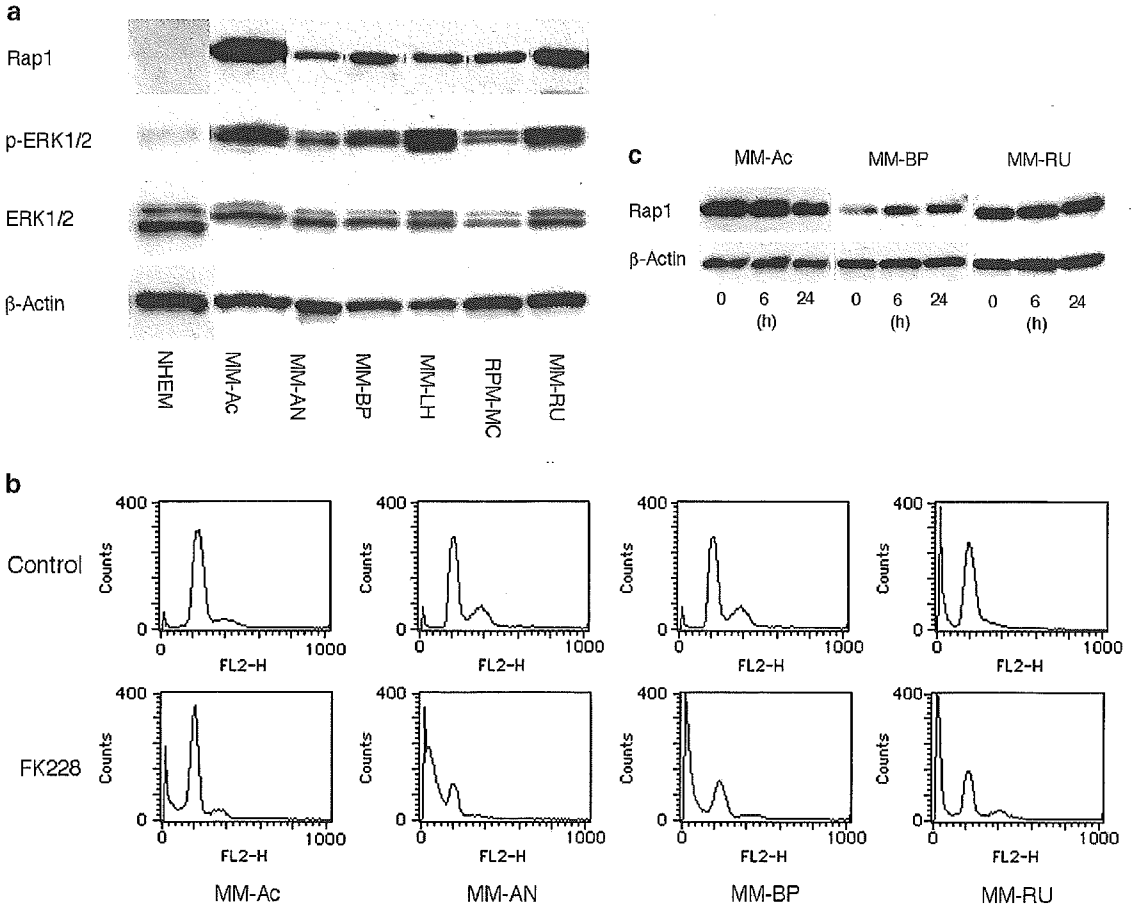

Figure 5 Expression of Rap1 and its relationship to FK228 sensitivity in melanoma cell lines. (**a**) Expression of Rap1, a phosphorylated species of ERK1/2, and ERK1/2 was examined in normal melanocytes (NHEM) and in six melanoma cell lines by immunoblotting. β-Actin expression served as a loading control. (**b**) MM-Ac, MM-AN, MM-BP, and MM-RU cells were cultured in the absence (Control) or presence (FK228) of 100 nM FK228 for 48 h, and were then subjected to flow cytometric analysis for cell cycle profiling. The quantified results are shown in Table 3. (**c**) Whole-cell lysates were prepared from MM-Ac, MM-BP, and MM-RU cells at the indicated time points, and subjected to immunoblotting for Rap1 and β-Actin expression.

Table 3 Cell cycle profile of FK228-treated melanoma cell lines

	Cell cycle profile[a]	*MM-AC*	*MM-AN*	*MM-BP*	*MM-RU*
Control	Sub-G1	4.6%	6.5%	2.4%	11.5%
	G0/G1	76.5%	67.8%	64.4%	75.1%
	S+G2/M	18.9%	25.7%	33.2%	13.4%
FK228	Sub-G1	19.3%	68.6%	57.3%	22.6%
	G0/G1	69.0%	24.2%	32.5%	54.6%
	S+G2/M	11.7%	7.2%	10.2%	22.8%

[a]The data shown in Figure 5b were quantified using the ModFit LT 2.0 program (Verity Software, Topsham, ME, USA).

Discussion

HDAC inhibitors are emerging as a new class of anticancer drugs (Melnick and Licht, 2002; Johnstone and Licht, 2003; Kim *et al.*, 2003). As the principle of their action differs from that of conventional chemotherapeutic agents, HDAC inhibitors are expected to be effective for treatment-resistant cancer including malignant melanoma. In this study, we found that the HDAC inhibitor FK228 was more effective against melanoma than other commonly used drugs such as adriamycin, vincristine, and interferon-β. FK228 almost completely suppressed cell growth and induced apoptosis in melanoma cells at $C_{max.}$, with less toxic effects on normal cells including melanocytes. These results are in line with recent studies using uveal melanoma cell lines (Klisovic *et al.*, 2003). Furthermore, we confirmed the antimelanoma effects of the drug *in vivo* using an animal model. Taken together, these findings appear to strongly encourage the clinical application of HDAC inhibitors, especially FK228, for malignant melanoma in the near future.

HDAC inhibitors are believed to exert cytotoxic effects by modulating transcription through the hyperacetylation of promoter regions. Target genes that have thus far been reported include cell cycle control elements (p21/Cip1, p27/Kip1, and cyclins A and D) (Sandor *et al.*, 2000; Derjuga *et al.*, 2001), apoptosis-inducing genes (Fas, Bax, and TNF) (Henderson *et al.*, 2003; Sutheesophon *et al.*, 2005), angiogenesis inhibitors (von

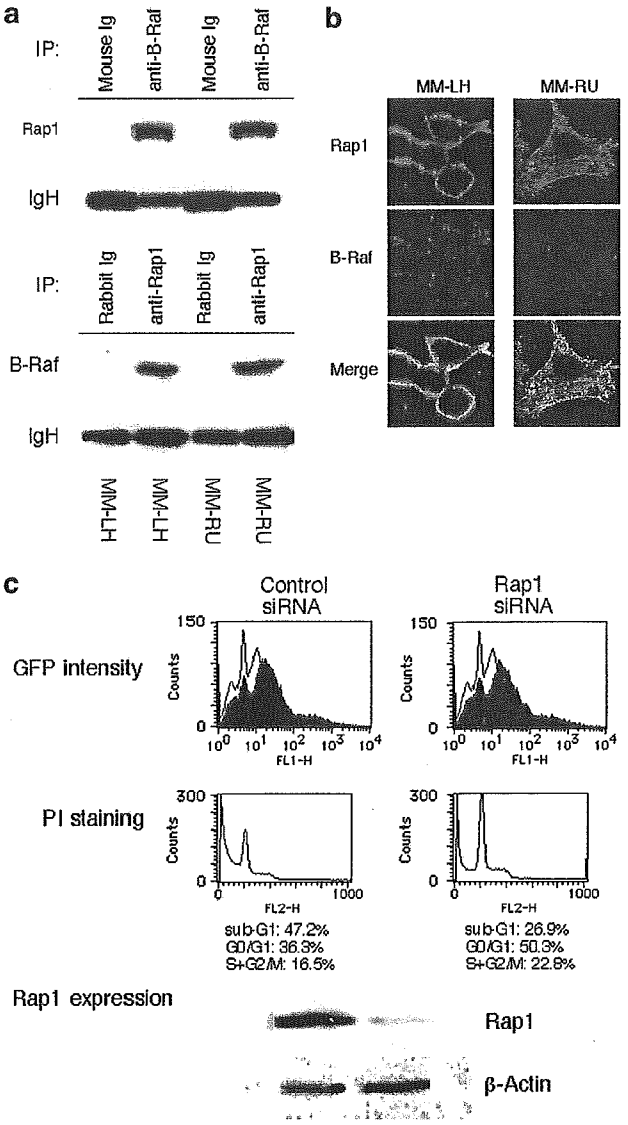

Figure 6 Intracellular association of Rap1 and B-Raf and its functional significance in melanoma cells. (**a**) Upper panel: Whole-cell lysates from MM-LH and MM-RU cells were subjected to immunoprecipitation with either preimmune mouse immunoglobulin (Mouse Ig) or anti-B-Raf monoclonal antibody, followed by immunoblotting with anti-Rap1 antibody. Lower panel: Whole-cell lysates from MM-LH and MM-RU cells were subjected to immunoprecipitation with either preimmune rabbit immunoglobulin (Rabbit Ig) or anti-Rap1 polyclonal antibody, followed by immunoblotting with anti-B-Raf antibody. Coomassie brilliant blue staining of the precipitated immunoglobulin heavy chain (IgH) is shown as a loading control. (**b**) MM-LH and MM-RU cells were double-stained with anti-Rap1 and anti-B-Raf antibodies as described in Materials and methods. (**c**) MM-RU cells were transfected with a pcPURU6βicassette vector containing either siRNA against Rap1 or a scrambled control, and were subjected to cell cycle analysis and Rap1 immunoblotting after 24 h.

Hippel-Lindau gene) (Kim *et al*., 2001), and adhesion molecules (CD86) (Maeda *et al*., 2000). In this study, we attempted to identify melanoma-specific target genes by comparing the gene expression profiles of melanoma cells and normal melanocytes. Seven genes fulfilled the criteria for FK228 effector genes, namely Silver-like (gp100/pMel17), TNF-α-induced protein 6, Rap1A, ADP-ribosylation factor 4, FLJ23028 (c-mer homolog), Coiled-coil forming protein 1, and TFIIB. We first pursued determination of the role of Rap1, a small GTP-binding protein of the Ras family, for two reasons. First, Rap1 is a regulator of Ras–MAP kinase signaling, which is altered in the vast majority of patients with melanoma. Second, Rap1A was originally isolated as Krev-1 by virtue of its ability to restore the malignant phenotype of activated Ras-transformed fibroblasts back to the normal phenotype (Kitayama *et al*., 1989), which is identical to the strategy used for the discovery of FK228 (Ueda *et al*., 1994). As anticipated, it was demonstrated that the cytotoxic effects of FK228 were at least in part mediated by the upregulation of Rap1A.

Recent investigations have revealed that abnormalities in the Ras–MAP kinase pathway are observed in most patients with malignant melanoma. Such abnormalities include activating mutations of N-Ras (4–30% of cases) (Omholt *et al*., 2003) and BRAF (40–70%) (Davies *et al*., 2002; Daniotti *et al*., 2004), and c-Raf hyperactivity (10%) (Wan *et al*., 2004). However, the significance of these abnormalities has not yet been firmly established; for example, benign melanocytic nevi is also associated with a high rate of mutation of the BRAF gene (Kumar *et al*., 2004). Nonetheless, it is believed that constitutive activation of Ras and/or Raf family kinases bypasses the requirement of growth factors and mitogenic stimuli, and serially activates MEK1/2, ERK1/2, and target molecules such as c-Myc and cyclin D, thereby leading to the deregulated proliferation of melanocytes (Satyamoorthy *et al*., 2003). The melanoma cell lines used in this study showed constitutive activation of this pathway via BRAF mutation in two lines, and c-Raf hyperactivation in one line. These abnormalities may be a target for therapeutic intervention, and the quest for isolation of the inhibitors of this pathway is currently underway in many laboratories (Karasarides *et al*., 2004). In this study, we found that FK228 suppressed the Ras–Raf–MEKK1/2–ERK1/2 pathway by upregulating Rap1 and downregulating Ras expression. The results of Rap1 overexpression and siRNA intervention suggest that Rap1 plays a major role in FK228-induced apoptosis, and the downregulation of Ras is also Rap1 dependent. Further investigation is required to elucidate the molecular basis of Rap1-mediated suppression of Ras expression, although translational or post-translational mechanisms are suggested in our study.

Rap1 is a small GTP-binding protein of the Ras family with the highest homology to Ras. It has two isoforms, Rap1A and Rap1B, with 95% homology, whose functional difference remains to be determined (Bokoch, 1993; Noda, 1993). In agreement with the method of isolation, several reports have provided evidence indicating that Rap1 antagonizes Ras signaling by trapping Ras effectors, in particular c-Raf, in an inactive complex (Kitayama *et al*., 1989; Cook *et al*., 1993; Hu *et al*., 1997). To date, the biological functions of Rap1 have been divided into two categories: (1) regulation of cell proliferation and (2) modulation of

integrin-mediated functions. The latter category includes cell-to-cell/extracellular matrix adhesion; cell polarity, movement, and migration; and phagocytosis (Tsukamoto *et al.*, 1999; Reedquist *et al.*, 2000; Schmidt *et al.*, 2001). Although the modulation of integrin-mediated processes by Rap1 may be related to the anti-invasive and antiangiogenic effects of HDAC inhibitors, this is beyond the scope of the present study. We instead focus on growth regulatory aspects of Rap1.

Our findings are compatible with earlier studies suggesting that Rap1 has both antiproliferative and antioncogenic potential (Kitayama *et al.*, 1989; Cook *et al.*, 1993; Hu *et al.*, 1997). In melanoma cells lacking BRAF mutation, FK228 easily suppressed the activation of Ras–MAP kinase signaling through the upregulation of Rap1, which in turn resulted in cell death. In contrast, the apoptosis-inducing effect of FK228 was relatively weak in melanoma cells with BRAF mutation, probably because of the high level of endogenous Rap1 expression. The present experiments with siRNA suggested that endogenous Rap1 acted to inhibit cell proliferation and viability by suppressing deregulated B-Raf activity. This finding appears to be somewhat contradictory to previous reports in which Rap1 was implicated in the activation of the ERK pathway by the direct binding and activation of B-Raf (Vossler *et al.*, 1997; York *et al.*, 1998). However, this observation was obtained in neuronal cells treated with cAMP, and was not reproduced in other cell types. For instance, cAMP-induced ERK activation is mediated by Ras rather than by Rap1 in melanocytes (Busca *et al.*, 2000). The function of Rap1 is therefore cell context dependent, and is determined by various factors. Growth regulation by Rap1 also varies according to cell type. For example, forced expression of Rap1A in normal T-cell clones induces an anergic state with compromised ERK1/2 activation in response to antigens (Boussiotis *et al.*, 1997; Katagiri *et al.*, 2002). In addition, D'Silva *et al.* (2003) reported that Rap1 expression increased during the growth arrest and differentiation of human keratinocytes, and the inactivation of Rap1 due to rapGAP overexpression resulted in enhanced proliferation. Loss-of-function mutations of DOCK-4, a specific Rap1 activator, have been detected in various human and murine tumor cells, suggesting that impaired activation of Rap1 can account for the overgrowth and invasive properties of some cancers (Yajnik *et al.*, 2003). In contrast, mice deficient for SPA-1, a member of the SPA-1 family Rap1 GAPs, develop an abnormal proliferation of myeloid cells resembling chronic myeloid leukemia (Ishida *et al.*, 2003). These results reinforce the notion that the role of Rap1 in cell proliferation is highly cell context dependent. Furthermore, some studies have suggested that Rap1B enhances cell growth upon overexpression (Altschuler and Ribeiro-Neto, 1998; Ribeiro-Neto *et al.*, 2002). It is possible that Rap1B acts in favor of cell proliferation, whereas Rap1A impairs cell growth and viability. Therefore, the balance between Rap1A and Rap1B may be important for cellular homeostasis, and the perturbation of this balance by the upregulation of Rap1A may be an underlying mechanism of the effects of FK228. We are currently conducting further experiments in order to evaluate this hypothesis.

Materials and methods

Cell lines and cell culture

The human melanoma cell lines MM-AN, MM-BP, MM-LH, MM-RU, and RPM-MC were kindly provided by Dr H Randolph Byers (Harvard Medical School). All cell lines were established from metastatic lymph nodes, except for RPM-MC, which originated in a recurrent primary lesion (Byers *et al.*, 1991). These cell lines were maintained in minimal essential medium (MEM) supplemented with 10% fetal calf serum (FCS), penicillin G, and streptomycin sulfate. MM-Ac (a gift of Dr Hiroshi Katayama, Katayama Dermatology Clinic, Gunma, Japan) was maintained in Dulbecco's modified Eagle's medium (DMEM) supplemented with 10% FCS, penicillin G, and streptomycin sulfate.

NHEM were purchased from Kurabo Biomedicals (Osaka, Japan), and grown in Medium154S supplemented with 10% FCS, basic fibroblast growth factor, hydrocortisone, insulin, transferrin, phorbol myristate acetate, heparin, and bovine pituitary extracts (Swope *et al.*, 1995). All cultures were carried out in a 5% CO_2 and 95% air humidified atmosphere at 37°C.

Animal experiments

Male C. B-17/Icr-SCID mice (6 weeks old) were purchased from CREA Japan Inc. (Tokyo, Japan) and maintained in containment level 2 cabinets with autoclaved food and water. MM-LH cells in exponential growth phase were harvested by trypsinization, and washed twice in PBS prior to injection. Animals were treated with anti-asialo GM1 antibody (Wako, Osaka, Japan) (200 μg/body) 1 day before tumor implantation, and 1×10^7 cells were injected subcutaneously into the abdominal skin of mice. After tumors were palpable (at day 6), animals were treated with either PBS or FK228 (0.5 mg/kg, intraperitoneally, every other day) (Skov *et al.*, 2003). Tumor growth was monitored by measurement of the two maximum perpendicular tumor diameters. All experiments in this study were performed in accordance with the Jichi Medical School Guide for Laboratory Animals.

Cell proliferation assays

Cells were harvested with trypsin, and resuspended in fresh medium containing the following test drugs: interferon-β, vincristine, adriamycin, and FK228. These drugs were provided by Mochida Pharmaceutical Co. (Tokyo, Japan), Shionogi Pharmaceutical Co. (Tokyo, Japan), Kyowa Hakko Co. (Osaka, Japan), and Fujisawa Pharmaceutical Co. (Osaka, Japan), respectively. An aliquot of 100 μl was placed in each well of 96-well plates, and the plates were then incubated at 37°C for 72 h. Cell proliferation was quantitatively assessed by BrdU incorporation using a BrdU assay kit (Roche Diagnostics, Mannheim, Germany).

Cell cycle analysis

The cell cycle profile was obtained by staining DNA with propidium iodide in preparation for flow cytometry analysis with the FACScan/CellQuest system (Becton-Dickinson, San Jose, CA, USA). The size of the sub-G1, G0/G1, and S + G2/M fractions was calculated as a percentage by analysing the DNA histograms using the ModFitLT 2.0 program (Verity Software, Topsham, ME, USA).

In situ *detection of apoptosis*
Apoptosis was detected *in situ* by TUNEL analysis using a MEBSTAIN apoptosis detection kit (MBL, Nagoya, Japan). The 3′-end of fragmented DNA of apoptotic cells was labeled with dUTP-FITC, giving off focal green fluorescent signals in the nuclei.

Plasmids and transfection
Rap1/Krev-1 expression plasmids, wild-type Rap1/Krev-1 and G12V active mutant, were constructed by inserting the corresponding full-length cDNAs into a pcDNA 3.1 vector (Invitrogen, Carlsbad, CA, USA). The G12V mutant is known to suppress the activity of Ras more efficiently than wild-type Rap1/Krev1 in some cell types (Kitayama *et al.*, 1990). An empty pcDNA 3.1 vector was used as a control. siRNA against Rap1 was subcloned into the pcPURU6βicassette siRNA expression vector (Takara Bio Co. Ltd, Shiga, Japan), expanded, and purified with an EndoFree plasmid purification kit (Qiagen Inc., Valencia, CA, USA). The target sequences of siRNA are as follows; TA0024-01, AGTCAAAGATCAA TGTTAA (nt 758); TA0024-02, AGCAGAAGATCGTCAG TAT (nt 278); TA0024-03, AGATCAATGTTAATGA GAT (nt 764). We used the scrambled sequences of each siRNA as controls. Transfection was carried out using LipofectAMINE 2000 transfection reagent (Invitrogen) according to the manufacturer's instructions. Transfection efficiency was assessed by cotransfection of the green fluorescent protein (GFP) expression vector pIRES2-EGFP (Clontech, Palo Alto, CA, USA). Upon flow cytometry and visual inspection, 20–30% of cells were found to be successfully transfected without significant variation among samples (data not shown).

Screening of the gene expression profile by DNA chip analysis
We cultured melanoma cell lines and NHEM in the absence or presence of 100 nM FK228 for 6 h, and isolated poly(A) RNA using a Poly(A) Quik mRNA isolation kit (Stratagene, La Jolla, CA, USA). Poly(A) RNAs from FK228-treated cells and the untreated control were labeled with Cy5 and Cy3, respectively, and hybridized to IntelliGene II human CHIP version 1.0 (Takara), which contains cDNA fragments of 3893 human cancer-related and cytokine genes. Precise information about the array is available at the manufacturer's website (http://www.takara.com). The cDNA array was scanned at 560 nm using the Affimetrix 428 Array Scanner, and the expression value for each gene was calculated as the average intensity difference using BioDiscovery ImaGene version 4.2 software. Expression values were normalized across the sample set by scaling the average of the fluorescent intensities of all genes on the array (Ferrando *et al.*, 2002).

Northern blotting
Total RNA was extracted from cells using an Isogen RNA extraction reagent (Nippon Gene, Toyama, Japan). A 15 μg portion of RNA samples was denatured with formaldehyde, and electrophoresed in a formaldehyde-agarose gel. RNA was then transferred onto nylon filters, and hybridized with Rap1A (Krev-1), Rap1B, and H-Ras cDNA probes, which were labeled with [^{32}P]dCTP using the Megaprime DNA labeling system (Amersham Pharmacia Biotech., Buckinghamshire, England), in Rapid-hyb buffer (Amersham Pharmacia Biotech.) for 1 h. The filters were washed once in 2 × SSC and 0.1% SDS at room temperature (RT) for 20 min, and three times in 0.1 × SSC and 0.1% SDS at 65°C for 15 min before being subjected to autoradiography. The signal intensities were quantified by densitometer.

Rap1A, Rap1B, and H-Ras cDNA fragments were prepared by PCR using the following primer pairs (D'Silva *et al.*, 2003): Rap1A (Krev-1), sense 5′-AATGTGACCTGGAAGATGAG CG-3′ and antisense 5′-AGGCAACAGTTCTTCATTCC-3′; Rap1B, sense 5′-TAGTCGTTCTTGGCTCAGGAGG-3′ and antisense 5′-AATGTGGACTGTGCTGTGATGG-3′; H-Ras, sense 5′-GGAAGCAGGTGGTCATTGATGG-3′ and antisense 5′-AGATTCCACAGTGCGTGC-3′. After 35 cycles of amplification at an annealing temperature of 60°C, PCR products were purified with a Wizard SV gel and PCR clean-up system (Promega, Madison, WI, USA).

Western blotting
For preparation of protein samples, cells were washed once with ice-cold phosphate-buffered saline, and were lysed on ice in cell lysis buffer (50 mM Tris-HCl, pH 8.0, 120 mM $NaCl_2$, 0.5% Nonidet P-40, 100 mM sodium fluoride, and 200 μM sodium orthovanadate) containing protease inhibitors. The particles were pelleted by centrifugation at 14 500 *g* for 15 min at 4°C. The supernatants were collected, and the protein contents were measured using a Bio-Rad protein assay kit (Bio-Rad, Richmond, CA, USA). Equal amounts of protein samples (20–40 μg) were electrophoresed on 10% SDS–polyacrylamide gels, and were then transferred onto Immobilon-P membranes (Millipore Corporation, Bedford, MA, USA). The membranes were incubated in 10% nonfat dry milk and 1% bovine serum albumin in Tris-buffered saline containing 0.05% Tween 20 (TBS-T) for 1 h at RT in order to avoid nonspecific protein binding. The membranes were placed in primary antibody solution for 1 h at RT or overnight at 4°C, depending on the antibody. The following primary antibodies were used: anti-Rap1 (121; Santa Cruz Biotechnology, Santa Cruz, CA, USA), anti-p21^{Ras} (clone 18; BD Transduction Laboratories, Lexington, KY, USA), anti-B-Raf (F-7; Santa Cruz Biotechnology), anti-phosphorylated c-Raf (Ser259) (Cell Signaling Technology, Beverley, MA, USA), anti-phosphorylated MEK1/2 (Ser217/221) (Cell Signaling Technology), anti-phosphorylated ERK1/2 (Thr202/Tyr204) (Cell Signaling Technology), anti-ERK1/2 (Cell Signaling Technology), anti-phosphorylated p38 MAP kinase (Thr180/Tyr182) (Cell Signaling Technology), anti-phosphorylated JNK (Thr183/Tyr185) (Cell Signaling Technology), and anti-β-actin (C4; ICN Biomedicals, Aurora, OH, USA). We used anti-rabbit or anti-mouse IgG linked to horseradish peroxidase (Amersham Corporation) as the second antibody, and an ECL enhanced chemiluminescence system (Amersham Corporation) for detection.

Immunoprecipitation/immunoblotting assays
After being precleared with protein G-Sepharose, whole-cell lysates (300 μg) were incubated with 2 μg of either anti-B-Raf antibody (F-7) or mouse IgG in 200 μl of cell lysis buffer. After brief centrifugation, the supernatants were rocked overnight at 4°C in the presence of protein G-Sepharose beads. Immune complexes were collected on the beads, washed three times in cell lysis buffer, and applied to 10% SDS–PAGE, followed by immunoblotting with anti-Rap1 antibody (sc-65). Reciprocal experiments were carried out according to the same protocol except that protein A-Sepharose and rabbit IgG were used instead of protein G-Sepharose and mouse IgG, respectively.

Confocal laser microscopy
The entire procedure was performed as described previously (Furukawa *et al.*, 2002). The cells were collected on glass slides using a Cytospin centrifugator (Shandon Scientific, Cheshire, UK), and fixed in 4% paraformaldehyde in PBS. Rap1 was

stained with anti-Rap1 polyclonal antibody (sc-65) and goat antibody to rabbit immunoglobulin conjugated with Alexa 488 (Molecular Probes, Eugene, OR, USA). B-Raf was stained with anti-B-Raf monoclonal antibody (F-7) and chicken antibody to mouse immunoglobulin conjugated with Cy3 (Amersham Biosciences).

Detection of BRAF mutations

DNA was isolated from melanoma cell lines according to the standard methods. Exons 11 and 15 of BRAF cDNA were amplified by PCR using the following primer pairs (Davies *et al.*, 2002): exon 11, sense 5′-TCCCTCTCSGGCATAAGG TAA-3′ and antisense 5′-CGAACAGTGAATATTTCCTTT GAT-3′; exon 15, sense 5′-TCATAATGCTTGCTCTGATA GGA-3′ and antisense 5′-GGCCAAAAATTTAATCAGTG GA-3′. The PCR products were subjected to direct DNA sequencing after purification.

Acknowledgements

We are grateful to Ms Noriko Hayashi and Ms Izumi Nozawa for their excellent technical assistance. We thank Drs Hideshi Ishii, Kazuhiro Ishikawa, Ken Futaki, and Taeko Wada (Jichi Medical School) for helpful discussions. This work was supported by High-Tech Research Center Project for Private Universities: Matching Fund Subsidy from MEXT 2002–2006, and by a grant from the Japan Medical Association (to YF).

References

Altschuler DL, Ribeiro-Neto F. (1998). *Proc Natl Acad Sci USA* **95**: 7475–7479.
Bokoch GM. (1993). *Biochem J* **289**: 17–24.
Boussiotis VA, Freeman GJ, Berezovskaya A, Barber DL, Nadler LM. (1997). *Science* **278**: 124–128.
Busca R, Abbe P, Mantoux F, Aberdam E, Peyssonnaux C, Eychene A *et al.* (2000). *EMBO J* **19**: 2900–2910.
Byers HR, Etoh T, Doherty JR, Sober AJ, Mihm MCJ. (1991). *Am J Pathol* **139**: 423–435.
Cook SJ, Rubinfeld B, Albert I, McCormick F. (1993). *EMBO J* **12**: 3475–3485.
Daniotti M, Oggionni M, Ranzani T, Vallacchi V, Campi V, Di Stasi D *et al.* (2004). *Oncogene* **23**: 5968–5977.
Davies H, Bignell GR, Cox C, Stephens P, Edkins S, Clegg S *et al.* (2002). *Nature* **417**: 949–954.
Derjuga A, Richard C, Crosato M, Wright PS, Chalifour L, Valdez J *et al.* (2001). *J Biol Chem* **276**: 37815–37820.
D'Silva NJ, Mitra RS, Zhang Z, Kurnit DM, Babcock CR, Polverini PJ *et al.* (2003). *J Cell Physiol* **196**: 532–540.
Ferrando AA, Neuberg DS, Staunton J, Loh ML, Huard C, Raimondi SC *et al.* (2002). *Cancer Cell* **1**: 75–87.
Francken AB, Shaw HM, Thompson JF, Soong SJ, Accortt NA, Azzola MF *et al.* (2004). *Ann Surg Oncol* **11**: 426–433.
Furukawa Y, Nishimura N, Furukawa Y, Satoh M, Endo H, Iwase S *et al.* (2002). *J Biol Chem* **277**: 39760–39768.
Furumai R, Matsuyama A, Kobashi N, Lee K-H, Nishiyama M, Nakajima H *et al.* (2002). *Cancer Res* **62**: 4916–4921.
Gore SD, Weng L-J, Figg WD, Zhai S, Donehower RC, Dover G *et al.* (2002). *Clin Cancer Res* **8**: 963–970.
Helmbach H, Rossmann E, Kern MA, Schadendorf D. (2001). *Int J Cancer* **93**: 617–622.
Henderson C, Mizzau M, Paroni G, Maestro R, Schneider C, Brancolini C. (2003). *J Biol Chem* **278**: 12579–12589.
Herman JG, Baylin SB. (2003). *N Engl J Med* **349**: 2041–2054.
Hong S-H, David G, Wong C-W, Dejean A, Privalsky ML. (1997). *Proc Natl Acad Sci USA* **94**: 9028–9033.
Hoshikawa Y, Kwon HJ, Yoshida M, Horinouchi S, Beppu T. (1994). *Exp Cell Res* **214**: 189–197.
Hu CD, Kariya K, Kotani G, Shirouzu M, Yokoyama S, Kataoka T. (1997). *J Biol Chem* **272**: 11702–11705.
Hubbard SR. (2004). *Cell* **116**: 764–766.
Ishida D, Kometani K, Yang H, Kakugawa K, Masuda K, Iwai K *et al.* (2003). *Cancer Cell* **4**: 55–65.
Johnstone RW, Licht JD. (2003). *Cancer Cell* **4**: 13–18.
Karasarides M, Chiloeches A, Hayward R, Niculescu-Duvaz D, Scanlon I, Friedlos F *et al.* (2004). *Oncogene* **23**: 6292–6298.
Katagiri K, Hattori M, Minato N, Kinashi T. (2002). *Mol Cell Biol* **22**: 1001–1015.
Kim DH, Kim M, Kwon HJ. (2003). *J Biochem Mol Biol* **36**: 110–119.
Kim MS, Kwon HJ, Lee YM, Baek JH, Jang J-E, Lee S-W *et al.* (2001). *Nat Med* **7**: 437–443.
Kitayama H, Matsuzaki T, Ikawa Y, Noda M. (1990). *Proc Natl Acad Sci USA* **87**: 4284–4288.
Kitayama H, Sugimoto Y, Matsuzaki T, Ikawa Y, Noda M. (1989). *Cell* **56**: 77–84.
Klisovic DD, Katz SE, Effron D, Klisovic MI, Wichbam J, Partburn MR *et al.* (2003). *Invest Ophthalmol Vis Sci* **44**: 2390–2398.
Kumar R, Angelini S, Snellman E, Hemminki K. (2004). *J Invest Dermatol* **122**: 342–348.
Lin RJ, Nagy L, Inoue S, Shao W, Miller Jr WH, Evans RM. (1998). *Nature* **391**: 811–814.
Maeda T, Towatari M, Kosugi H, Saito H. (2000). *Blood* **96**: 3847–3856.
Marks P, Rifkind RA, Richon VM, Breslow R, Miller T, Kelly WK. (2001). *Nat Rev Cancer* **1**: 194–202.
Melnick A, Licht JD. (2002). *Curr Opin Hematol* **9**: 322–332.
Nakajima H, Kim YB, Terano H, Yoshida M, Horinouchi S. (1998). *Exp Cell Res* **241**: 126–133.
Noda M. (1993). *Biochim Biophys Acta* **1155**: 97–109.
Omholt K, Platz A, Kanter L, Ringborg U, Hansson J. (2003). *Clin Cancer Res* **9**: 6483–6488.
Reedquist KA, Ross E, Koop EA, Wolthuis RM, Zwartkruis FJ, van Kooyk Y *et al.* (2000). *J Cell Biol* **148**: 1151–1158.
Ribeiro-Neto F, Urbani J, Lemee N, Lou L, Altschuler DL. (2002). *Proc Natl Acad Sci USA* **99**: 5418–5423.
Sandor V, Bakke S, Robery RW, Kang MH, Blagosklonny MV, Bender J *et al.* (2002). *Clin Cancer Res* **8**: 718–728.
Sandor V, Senderowicz A, Mertins S, Sackett D, Sausville E, Blagosklonny MV *et al.* (2000). *Br J Cancer* **83**: 817–825.
Satyamoorthy K, Li G, Gerrero MR, Brose MS, Volpe P, Weber BL *et al.* (2003). *Cancer Res* **63**: 756–759.
Schmidt A, Caron E, Hall A. (2001). *Mol Cell Biol* **21**: 438–448.
Skov S, Rieneck K, Bovin LF, Skak K, Tomra S, Michelsen BK *et al.* (2003). *Blood* **101**: 1430–1438.
Soengas MS, Lowe SW. (2003). *Oncogene* **22**: 3138–3151.
Somech R, Izraeli S, Simon AJ. (2004). *Cancer Treat Rev* **30**: 461–472.
Sutheesophon K, Nishimura N, Kobayashi Y, Furukawa Y, Kawano M, Itoh K *et al.* (2005). *J Cell Physiol* **203**: 387–397.

Swope VB, Medrano EE, Smalara D, Abdel-Malek ZA. (1995). *Exp Cell Res* **217**: 453–459.
Tsukamoto N, Hattori M, Yang H, Bos JL, Minato N. (1999). *J Biol Chem* **274**: 18463–18469.
Ueda H, Nakajima H, Hori Y, Fujita T, Nishimura M, Goto T *et al.* (1994). *J Antibiot (Tokyo)* **47**: 301–310.
Vossler MR, Yao H, York RD, Pan MG, Rim CS, Stork PJ. (1997). *Cell* **89**: 73–82.
Wan PTC, Garnett MJ, Roe SM, Lee S, Niculescu-Duvaz D, Good VM *et al.* (2004). *Cell* **116**: 855–867.
Yajnik V, Paulding C, Sordella R, McClatchey AI, Saito M, Wahrer DC *et al.* (2003). *Cell* **112**: 673–684.
York RD, Yao H, Dillon T, Ellig CL, Eckert SP, McCleskey EW *et al.* (1998). *Nature* **392**: 622–626.
Zhu P, Martin E, Mengwasser J, Schlag P, Janssen K-P, Gottlicher M. (2004). *Cancer Cell* **5**: 455–463.

JOURNAL OF CELLULAR PHYSIOLOGY 203:387–397 (2005)

Involvement of the Tumor Necrosis Factor (TNF)/TNF Receptor System in Leukemic Cell Apoptosis Induced by Histone Deacetylase Inhibitor Depsipeptide (FK228)

KRITTAYA SUTHEESOPHON,[1,2] NORIKO NISHIMURA,[1] YUKIKO KOBAYASHI,[1] YUTAKA FURUKAWA,[1] MIKIHIKO KAWANO,[2] KOUICHI ITOH,[2] YASUHIKO KANO,[3] HIDESHI ISHII,[1] AND YUSUKE FURUKAWA[1]*

[1]*Division of Stem Cell Regulation, Center for Molecular Medicine, Jichi Medical School, Tochigi, Japan*
[2]*Department of Laboratory Medicine, Jichi Medical School, Tochigi, Japan*
[3]*Division of Medical Oncology, Tochigi Cancer Center, Tochigi, Japan*

Inhibition of histone deacetylase (HDAC) is a novel strategy for the treatment of leukemias via restoration of aberrantly silenced genes. In this study, we conducted a detailed analysis of anti-leukemic effects of an HDAC inhibitor (HDI), depsipeptide (FK228), using myeloid leukemia cell lines HL-60 and K562. DNA chip analysis revealed upregulation of TNF-α mRNA and a number of molecules involved in TNF-signaling such as TRAF-6, caspases-10, and -7 in depsipeptide-treated HL-60 cells, which prompted us to examine the involvement of the TNF/TNF receptor system in the anti-leukemic effects of the drug. Upregulation of TNF-α was induced by depsipeptide in HL-60 and K562 cells, which expressed type I TNF receptors (TNF-RI). Depsipeptide activated caspases-8 and -10, which in turn cleave caspases-3 and -7, leading to apoptotic cell death in both cell lines. Anti-TNF-α neutralizing antibody and short interfering RNA (siRNA) against TNF-RI alleviated the activation of the caspase cascade and the induction of apoptosis, indicating the presence of an autocrine loop. Finally, we demonstrated that the enhanced production of TNF-α by depsipeptide was due to transcriptional activation of the TNF-α gene through hyperacetylation of histones H3 and H4 in its promoter region (−208 to +35). These results suggest that autocrine production of TNF-α plays a role in the cytotoxicity of depsipeptide against a subset of leukemias. J. Cell. Physiol. 203: 387–397, 2005. © 2004 Wiley-Liss, Inc.

Modifications of core histone tails are implicated in the regulation of gene transcription. Accumulating evidence suggests that acetylation and deacetylation are particularly important among them, and the balance between the two processes defines the status of transcription of most eukaryotic genes (Jenuwein and Allis, 2001). Histone acetylation triggers the initiation of gene transcription by recruiting chromatin remodeling factors and the general transcription machinery to promoter regions (Agalioti et al., 2002). In contrast, histone deacetylation acts in favor of gene silencing and contributes to the formation of transcriptionally inactive heterochromatin in concert with histone methylation (Nakayama et al., 2001).

Histone deacetylation is mediated by a group of enzymes collectively known as histone deacetylases (HDACs) (Khochbin et al., 2001). Recently, it has been shown that HDACs are involved in leukemogenesis. Various leukemic fusion proteins, including PML/RARα, PLZF/RARα, AML-1/ETO, and CBFβ/MYH11, form a complex with HDACs with higher affinities than their normal counterparts, which aberrantly suppresses the expression of genes required for cell differentiation and growth control, leading to the transformation of primitive hematopoietic cells (Hong et al., 1997; Lin et al., 1998).

Given the role of HDACs in leukemogenesis, the use of HDAC inhibitors (HDIs) is expected to set a novel strategy for the treatment of leukemia called "transcription therapy" (Minucci et al., 2001; Melnick and Licht, 2002; Johnstone and Licht, 2003). HDIs can restore the expression of genes aberrantly suppressed in leukemic cells, which may result in cell cycle arrest, differentiation, and apoptosis. Indeed, HDIs had cytotoxic effects on leukemic cell lines (Murata et al., 2000) and primary cells from patients with chronic lymphocytic leukemia in vitro (Byrd et al., 1999). Furthermore, Ueda et al. (1994) reported that HDIs could prolong the life of mice-bearing transplanted tumors including P388 and L1210 leukemias. Currently, phase I and II clinical trials are ongoing for four different types of HDIs, sodium phenylbutyrate, depsipeptide (FK228), suberoylanilide hydroxamic acid (SAHA), and MS-275, in hematologic malignancies and various solid tumors (Gore et al., 2002; Sandor et al., 2002). Among these compounds, depsipeptide (FK228) is especially promising in the field of clinical hematology, because this agent is reported to exhibit significant therapeutic effects in patients with T-cell lymphoma with minimal toxicity (Piekarz et al., 2001). For safe and effective clinical applications, however, it is essential to clarify the molecular basis of the cytotoxic activity of this drug. Unfortunately, relatively little is known about the mechanisms of the cytotoxic effects of HDIs on leukemias compared with solid tumors. In this study, with this background in mind, we investigated the mechanisms of

Contract grant sponsor: Ministry of Education, Science and Culture of Japan; Contract grant sponsor: Japan Leukemia Research Fund.

*Correspondence to: Yusuke Furukawa, Division of Stem Cell Regulation, Center for Molecular Medicine, Jichi Medical School, 3311-1 Yakushiji, Minamikachi-machi, Tochigi 329-0498, Japan. E-mail: furuyu@jichi.ac.jp

Received 5 March 2004; Accepted 2 September 2004

Published online in Wiley InterScience (www.interscience.wiley.com.), 28 October 2004.
DOI: 10.1002/jcp.20235

the anti-leukemic effects of depsipeptide (FK228) using HL-60 and K562 leukemia cell lines.

MATERIALS AND METHODS

Reagents

All chemicals were purchased from Sigma Chemical Co. (St. Louis, MO) unless otherwise stated. Depsipeptide (FK228) was provided by Fujisawa Pharmaceutical Co. Ltd. (Osaka, Japan), dissolved in dimethylsulfoxide at 2 mM, and stored at −20°C until use. We obtained short interfering RNA (siRNA) against the type I TNF receptor (TNF-RI) and its control from Santa Cruz Biotechnology (Santa Cruz, CA), and used according to the manufacturer's protocol.

Cells and cell culture

We purchased human myeloid leukemia cell lines, HL-60 and K562, from American Type Culture Collection (ATCC; Manassas, VA). These cell lines were maintained in RPMI1640 medium supplemented with 10% fetal bovine serum.

Flow cytometry

The cell cycle profile was obtained by staining DNA with propidium iodide in preparation for flow cytometry with the FACScan/CellQuest system (Becton-Dickinson, San Jose, CA). The size of the sub-G1, G0/G1, and S+G2/M fractions was calculated as a percentage by analyzing DNA histograms with the ModFitLT 2.0 program (Verity Software, Topsham, ME). Surface expression of the TNF receptor was detected using a specific antibody against TNF-RI (MABTNFR1-B1; BD Biosciences Pharmingen, San Jose, CA) according to the standard protocol. We used purified mouse IgG as an isotype-matched control. Cells in the early phases of apoptosis were detected by annexin V staining (Annexin V-FITC apoptosis detection kit; MBL, Nagoya, Japan).

Enzyme-linked immunosorbent assay (ELISA)

We measured the amounts of TNF-α protein in the conditioned medium of HL-60 and K562 cells using the TNF-α ELISA kit (R&D systems, Minneapolis, MN).

Screening of gene expression profile by DNA chip analysis

We cultured HL-60 cells in the absence or presence of 20 nM depsipeptide (FK228) for 6 h, and isolated poly (A) RNA using a Poly (A) Quik mRNA isolation kit (Stratagene, La Jolla, CA). Poly (A) RNAs from depsipeptide-treated cells and the untreated control were labeled with Cy5 and Cy3, respectively, and hybridized to IntelliGene human cancer CHIP version 3.0 (Takara Bio Co. Ltd., Shiga, Japan), which contains cDNA fragments of 641 known cancer-related genes. Precise information of the array is available at the company's website (http://www.takara-bio.co.jp). The cDNA array was scanned at 560 nm using the Affimetrix 428 Array Scanner. The results were analyzed with BioDiscovery ImaGene version 4.2 software.

Northern blotting

An equal amount (15 μg) of total cellular RNA was electrophoresed in 1% agarose gels containing formaldehyde, and blotted onto Hybond N^+ synthetic nylon membranes (Amersham Pharmacia Biotech., Buckinghamshire, England). The membranes were hybridized with ^{32}P-labeled probes in Rapid-hyb buffer (Amersham Pharmacia Biotech.). We used a 1.1-kb full-length TNF-α cDNA (Wang et al., 1985), a 801 bp PCR fragment of type I TNF receptor cDNA (nt. 1213–2013) (Fuchs et al., 1992), a 1.4-kb full-length IL-1β cDNA (provided by Ajinomoto Pharmaceutical, Co., Tokyo, Japan), and a 598 bp PCR fragment of glyceraldehyde-3-phosphate dehydrogenase (GAPDH) cDNA (nt. 146–743) as probes.

Western blotting

Immunoblotting was carried out according to the standard method using the following antibodies: anti-type I TNF receptor (H-5; Santa Cruz Biotechnology), anti-procaspase-8 (B9-2; BD Pharmingen), anti-cleaved caspase-8 (11G10; Cell Signaling Technology, Beverley, MA), anti-procaspase-10 (#9752; Cell Signaling Technology), anti-procaspase-3 (clone 97; BD Transduction Laboratories, Lexington, KY), anti-cleaved caspase-3 (#9661; Cell Signaling Technology), anti-cleaved caspase-7 (#9492; Cell Signaling Technology), anti-poly(ADP-ribose) polymerase (PARP) (4C10-5; BD Pharmingen), anti-ASK1 (#3761; Cell Signaling Technology), anti-phosphorylated JNK (#9251; Cell Signaling Technology), and anti-β-actin (C4; ICN Biomedicals, Aurora, OH). The inhibition of HDACs by depsipeptide (FK228) was monitored with specific antibodies recognizing histones acetylated at the following sites: lysine 9 of histone H3 (H3-K9), lysine 18 of histone H3 (H3-K18), lysine 8 of histone H4 (H4-K8), and lysine 12 of histone H4 (H4-K12) (all purchased from Cell Signaling Technology).

Nuclear run-on assay

HL-60 cells were cultured in the absence or presence of 20 nM depsipeptide (FK228) for 6 h. After being washed with phosphate-buffered saline, cells were disrupted in cell lysis buffer (10 mM Tris HCl, pH 8, 40 mM NaCl, 1.5 mM $MgCl_2$, and 0.02% nonidet P-40) containing protease inhibitor complex (Roche Diagnostics, Mannheim, Germany) on ice for 10 min, and nuclei were collected by microcentrifugation. Nascent nuclear RNA was transcribed in labeling buffer (20 mM Tris HCl, pH 8, 140 mM KCl, 10 mM $MgCl_2$, 1 mM $MoCl_2$, 20% glycerol, 14 mM β-mercaptoethanol, 10 mM phosphocreatine, 100 μg/mL phosphocreatine kinase, and 1 mM each of ATP, GTP and CTP) in the presence of 1 mCi/mL [^{32}P]UTP for 20 min at 30°C. The elongated RNA was purified after DNase and proteinase K treatment, and hybridized to immobilized plasmids containing cDNAs for TNF-α, β-globin, and GAPDH at 1×10^6 cpm/mL as previously described (Furukawa et al., 1990).

Chromatin immunoprecipitation (ChIP) assay

The ChIP assay was performed as reported (Furukawa et al., 2002) with some modifications. Approximately 1×10^6 cells were resuspended in PBS, fixed with 1% formaldehyde at 37°C for 10 min, resuspended in 200 μL of SDS-lysis buffer (50 mM Tris HCl, pH 8, 10 mM EDTA, and 1% SDS), and sonicated on ice with 10-sec pulses 4× to disrupt chromatin at an average length of 500–1,000 bp. Sonicated cell suspensions were centrifuged at 13,000 rpm for 10 min, and 20 μL of each supernatant was heated at 65°C for 4 h after the addition of 0.8 μL of 5 M NaCl, which was used as an input. The rest of the supernatant was added to 1.8 mL of ChIP dilution buffer (167 mM NaCl, 16.7 mM Tris HCl, pH 8, 1.2 mM EDTA, 0.01% SDS, 1.1% Triton X-100, 20 μg/mL salmon sperm DNA, and 50 μg/mL yeast tRNA) containing 10 μg of either anti-acetylated histone H3 antibody or anti-acetylated histone H4 antibody (Upstate Biotechnology, Lake Placid, NY). After incubation at 4°C for 16 h, the mixtures were further rocked with 60 μL of protein A agarose beads in the presence of BSA at 15 μg/mL and salmon sperm DNA at 12 μg/mL for 1 h. The immunoprecipitates were washed 3× each with four different buffers, then eluted with 0.1 M $NaHCO_3$ and 1% SDS. The eluents were heat-treated, digested with proteinase K, extracted with phenol/chloroform, ethanol-precipitated, and finally resuspended in 20 μL of TE (pH 8). We used 5 μL of the final suspension for PCR amplification of the promoter region of the TNF-α gene (−208 to +35) (Takashiba et al., 1993). The primer sequences are 5′-TATCCTTGATGCTTGTGTGTCC-3′ for the sense primer and 5′-CTCTGCTGTCCTTGCTGAGGGA-3′ for the antisense primer. In pilot experiments, we found 30 cycles to be the number most suitable for quantitative detection of the PCR product.

RESULTS

Screening of the changes in gene expression in depsipeptide-treated HL-60 cells

Because the principal action of HDIs is the modulation of transcription, it is reasonable to screen for changes in gene expression as an initial step in exploring the mechanisms of the cytotoxic effects of depsipeptide (FK228). To set optimal conditions for gene expression

analysis, we first determined the time-course of the effects of depsipeptide (FK228) using the human myeloid leukemia cell line HL-60. Cell cycle analysis was serially performed with HL-60 cells cultured in the absence or presence of depsipeptide (FK228) at a concentration of 20 nM, defined as the optimal concentration for myeloid leukemic cells in our pilot study (Kano, Y. et al., manuscript in preparation) and 50× lower than the C_{max} of the drug (Sandor et al., 2002). As shown in Figure 1A, depsipeptide (FK228) induced cell cycle arrest at G2/M phase of the cell cycle after 24 h, followed by the appearance of sub-G1 fraction at 48 h of culture. The time course of the response to the drug was almost the same in K562 cells (data not shown). To confirm the induction of apoptosis by depsipeptide (FK228), we performed annexin V staining for depsipeptide-treated HL-60 cells. As shown in Figure 1B, annexin V-positive cells appeared after 24 h of culture, indicating that depsipeptide (FK228) causes apoptosis in leukemic cells.

According to this result, we decided to perform a DNA chip analysis using RNA samples isolated at 6 h of culture, at which time point no significant changes appeared on DNA histograms. The results of the analysis are summarized in Table 1—eight genes showed more than 2.5-fold increase in mRNA expression compared with the untreated control, and 12 genes showed more than twofold decrease among 641 cancer-related genes screened. It is of note that TNF-α mRNA expression was upregulated approximately threefold, and TNF-activated caspases (caspases-7 and -10) and TNF-related genes (TRAF-6, TNF2, TNF10, and TNF10b receptor) were included in the genes detected after depsipeptide treatment (data not shown). These results suggest the involvement of the TNF/TNF receptor system in the anti-leukemic effects of depsipeptide (FK228).

Effects of depsipeptide (FK228) on the expression of TNF-α and its receptor in leukemic cells

To confirm the upregulation of TNF-α by depsipeptide (FK228), we carried out Northern blotting using HL-60 and K562 cell lines. Consistent with the result of the DNA chip analysis, the abundance of TNF-α transcript increased approximately three- and fivefold in depsipeptide-treated HL-60 and K562 cells, respectively, whereas no change was observed in the untreated control (Fig. 2A and data not shown). We then examined the production of TNF-α protein of these cells using ELISA. As shown in Table 2, TNF-α protein in the supernatants was below the detection limits in untreated HL-60 and K562 cells, but detectable after depsipeptide treatment, indicating that the increase in mRNA expression actually resulted in enhanced TNF-α protein production. To show the specificity of our observation, we reprobed the membrane filter with interleukin-1β probe. No changes were noted in the levels of IL-1β mRNA expression (Fig. 2A), suggesting that the upregulation of TNF-α is not part of the general increase in transcription of cytokine genes by depsipeptide (FK228).

Next, we investigated the presence of TNF-α receptors on these cell lines. As shown in Figure 2A, the type I TNF receptor (TNF-RI) mRNA was highly expressed in untreated HL-60 and K562 cells, and was downregulated after 12 h of treatment with depsipeptide (FK228). We then carried out flow cytometric and immunoblot analyses using specific antibodies against TNF-RI to confirm the expression of TNF receptors on HL-60 and K562 cells. TNF receptors were constitutively expressed on these cells, and were not affected by depsipeptide

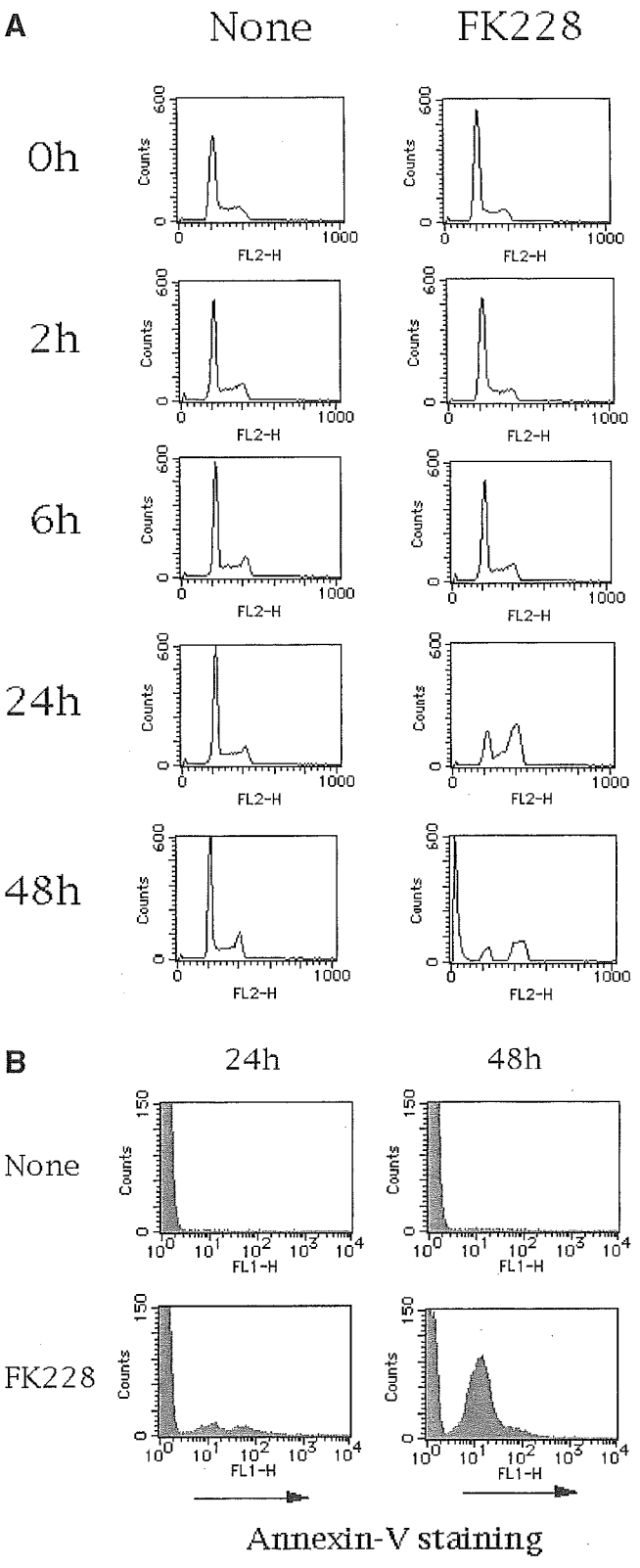

Fig. 1. Depsipeptide (FK228) induced cell cycle arrest and apoptosis in HL60 cells. HL-60 cells were cultured in the absence (none) or presence of depsipeptide (FK228) at a final concentration of 20 nM for up to 48 h. Cells were harvested at the indicated time points, and stained with propidium iodide for cell cycle analysis (**A**) and annexin V-FITC for the detection of apoptosis (**B**) by flow cytometry. The data shown are representative of multiple independent experiments.

TABLE 1. Results of DNA chip analysis of depsipeptide-treated HL60 cells

Category	Gene name	Accession[a]	Fold changes
Genes whose expression was increased by FK228	c-fyn	AJ310436	4.71
	Proteasome subunit β9	NM002800	4.28
	Glutaredoxin (thioltransferase)	NM002064	3.49
	Lysozyme	NM000239	3.40
	TNF-α	NM004862	2.97
	IFNγ-inducible protein 30	NM006332	2.83
	PMA-induced protein-1	NM021127	2.78
	NF-IL3	NM005384	2.76
Genes whose expression was decreased by FK228	CHED	AJ297709	−2.58
	Wee1	X62048	−2.46
	Ikaros	NM006060	−2.45
	A kinase (PRKA) anchor protein 1	NM003488	−2.36
	RB-binding protein 6	NM006910	−2.32
	BCR-related gene	NM021962	−2.28
	CD11a	NM002209	−2.28
	ATM	U82828	−2.25
	Lymphoid-restricted membrane protein	NM006152	−2.23
	ATP-dependent DNA ligase III	NM013975	−2.22
	Ki-67	X65550	−2.21
	CDC7-like 1	NM003503	−2.20

[a]Poly(A) RNAs were isolated from HL-60 cells treated with 20 nM depsipeptide for 6 h and from the untreated control, labeled with Cy5 and Cy3, respectively, and hybridized to IntelliGene human cancer CHIP version 3.0 (Takara), which contains cDNA fragments of 641 cancer-related genes. Precise information of the array is available at the company's website (http://www.takara.com).

(FK228) at 12–24 h of culture, when TNF-α production was maximal at both mRNA and protein levels (Fig. 2B,C, and Table 3).

Autocrine activation of the TNF-signaling pathway in depsipeptide-treated leukemic cells

The production of TNF-α in and the expression of its receptor on depsipeptide-treated HL-60 and K562 cells support the notion that TNF-α acts on these cells in an autocrine or paracrine manner to trigger apoptosis. To substantiate this hypothesis, we first investigated whether the TNF-signaling pathway is really activated in depsipeptide-treated leukemic cells. It is well known that, among initiator caspases, caspases-8 and -10 are cleaved and activated in the death-inducing signaling complex (DISC) formed upon the engagement of TNF-α to type I TNF receptors (Barnhart and Peter, 2003). The activated caspases-8 and -10, in turn, cleave executioner caspases such as caspases-3 and -7 (Budihardjo et al., 1999). Based on this knowledge, we examined the expression of these caspases using immunoblotting. As shown in Figure 3, the amounts of procaspases-8, -10, and -3 readily decreased and cleaved caspases-8, -3, and -7 appeared in HL-60 cells after 24 h of culture with depsipeptide (FK228), whereas no such changes were detected in the untreated control. Similar results were obtained with K562 cells (data not shown). Furthermore, the cleavage of PARP, a substrate of caspase-3, was observed after 48 h of the treatment, indicating that caspases were really activated in depsipeptide-treated cells (Fig. 3).

To obtain direct evidence that autocrine TNF-α mediates the activation of the caspase cascade and subsequent apoptosis, we examined the effect of anti-TNF-α neutralizing antibody on the cytotoxicity of depsipeptide (FK228) against HL-60 cells. Anti-TNF-α antibody alleviated the depsipeptide-induced apoptosis of HL-60 cells (a representative result is shown in Fig. 4A, and the results of three independent experiments are summarized in Table 4) as well as the activation of caspase-8 (Fig. 4B). In addition, we also examined whether siRNA-mediated targeting of TNF receptors affected the cytotoxic effects of depsipeptide (FK228). As shown in Figure 4C, siRNA against TNF-RI but not control siRNA suppressed FK228-induced apoptosis in accord with the reduction of TNF-RI expression. It is of note that the residual cells did not show an accumulation at G2/M phase, suggesting that autocrine TNF-α also plays a role in cell cycle arrest. Taken together, these results indicate that depsipeptide (FK228) induces production of TNF-α in certain subsets of myeloid leukemia cells, which in turn activates TNF receptor-mediated signal transduction pathways in an autocrine or paracrine manner, leading to apoptotic cell death and possibly cell cycle arrest.

In addition to the activation of the caspase cascade, TNF receptors appear to transduce death signals via a second pathway involving the Jun kinase cascade: ASK1-MKK4/7-JNK (c-Jun N-terminal kinase) (Baker and Reddy, 1998). We, therefore, investigated whether depsipeptide (FK228) simultaneously activated this pathway to induce apoptosis in leukemic cells. As shown in Figure 5, however, FK228 failed to activate JNK probably because of downregulation of its upstream activator ASK1.

Depsipeptide (FK228) activates transcription of the TNF-α gene through hyperacetylation of its promoter

Finally, we investigated the mechanisms of upregulation of TNF-α mRNA by depsipeptide (FK228). First, we examined whether the enhanced expression of TNF-α mRNA is mediated through transcriptional or post-transcriptional mechanisms. Nuclear run-on assays revealed that transcription of the TNF-α gene was significantly augmented in depsipeptide-treated HL-60 cells (Fig. 6). Because the increase in TNF-α transcription is more than tenfold after adjusting to GAPDH transcription levels, upregulation of TNF-α mRNA can be explained solely by transcriptional activation, although the involvement of post-transcriptional mechanisms is not entirely excluded.

To clarify the mechanisms of transcriptional activation of the TNF-α gene by depsipeptide (FK228), we analyzed the status of histone acetylation in the TNF-α promoter using ChIP assays. Before going on to ChIP

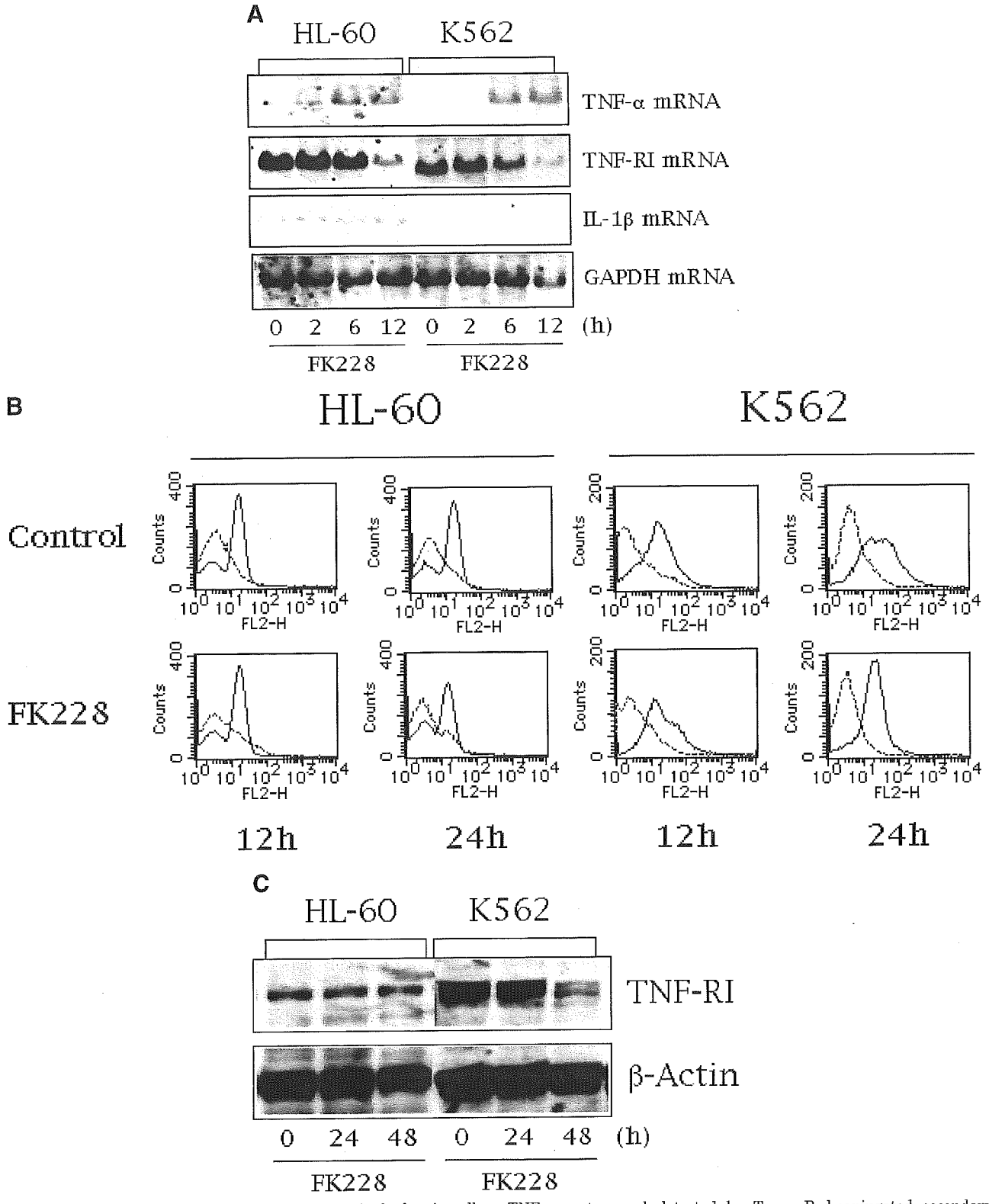

Fig. 2. Expression of TNF-α and its receptors in leukemic cells treated with depsipeptide (FK228). **A**: HL-60 and K562 cells were cultured with 20 nM depsipeptide (FK228) for up to 12 h. Total cellular RNA was isolated at the indicated time points, and subjected to Northern blot analysis for mRNA expression of TNF-α, TNF-RI, and IL-1β. The membrane filters were reprobed with GAPDH cDNA to serve as a loading control. **B**: TNF receptors on the surface of HL-60 and K562 cells were stained with a specific antibody against type I TNF receptor, and detected by Texas Red-conjugated secondary antibody using flow cytometry (straight lines). Purified mouse IgG was used as an isotype-matched control (dotted lines). **C**: Whole cell lysates were prepared from depsipeptide-treated HL-60 and K562 cells, and subjected to immunoblot analysis for TNF-RI expression. The membrane filters were reprobed with anti-β-actin antibody to verify the equal loading and integrity of samples. The data shown are representative of multiple independent experiments.

TABLE 2. TNF-α production in FK228-treated cells

Cell line	HL-60				K562			
Incubation time	12 h		24 h		12 h		24 h	
FK228	(−)	(+)	(−)	(+)	(−)	(+)	(−)	(+)
TNF-α[a]	<5.0	5.6 ± 2.4	<5.0	18.0 ± 4.8	<5.0	7.9 ± 1.7	<5.0	12.8 ± 3.1

[a]The amounts of TNF-α in the supernatants determined by ELISA (pg/mL; mean ± SD, n = 3).

assays, we confirmed the effects of depsipeptide (FK228) as an HDI in vivo. As shown in Figure 7A, depsipeptide treatment caused the hyperacetylation of N-terminal lysine residues of histones H3 and H4 after 2 h of treatment in HL-60 cells. Previous studies have demonstrated that transcription of the TNF-α gene is governed by the formation of stimuli-specific enhancer complexes on its minimal promoter region between nucleotides -200 and -20 (Falvo et al., 2000). Notably, it has been shown that the enhancer complexes contain histone acetyltransferases CBP/p300, implying the importance of histone acetylation in the transcriptional regulation of TNF-α (Barthel et al., 2003). We, therefore, performed ChIP assays using specific antibodies against acetylated histones H3 and H4, and found that both histones were inducibly acetylated in the core promoter regions of the TNF-α gene after 2 h of culture with depsipeptide in HL-60 cells (Fig. 7B). These findings indicate that depsipeptide (FK228) enhances transcription of the TNF-α gene through hyperacetylation of its promoter.

DISCUSSION

Given the anticipated role of HDIs in cancer treatment, it is essential to clarify their mechanisms of action in detail for better clinical applications in the future. Evidence is accumulating regarding the cellular consequences of HDI treatment for cancer, which include cell cycle arrest (Qiu et al., 2000), apoptosis (Bernhard et al., 1999), cellular differentiation (Warrell et al., 1998), suppression of tumor angiogenesis (Kim et al., 2001), and immunomodulation (Maeda et al., 2000). The molecular basis of these phenomena has also been studied extensively using conventional methods as well as global gene expression analysis. For example, HDIs accumulate target cells at either G1 or G2/M phase of the cell cycle, depending on the status of p53, through transcriptional activation of a CDK inhibitor, p21/Cip1 (Richon et al., 2000; Derjuga et al., 2001). HDI-induced cell cycle arrest may also be mediated by the altered expression of cyclin A, cyclin D, and p27/Kip1, resulting in a reduction in CDK2 and CDK4 activities (Sandor et al., 2000). As for apoptosis, the transcriptional activation of proapoptotic genes such as Fas and Bax is proposed to mediate HDI-induced apoptosis (Kwon et al., 2002). Other possible mechanisms of apoptosis include the perturbation of mitochondrial membranes, which results in the release of cytochrome *c* and subsequent activation of caspase-9 (Henderson et al., 2003), modulation of the expression of Bcl-2 family proteins (Amin et al., 2001), and the generation of reactive oxygen species (Ruefli et al., 2001). However, these findings were obtained using different HDIs in various cell systems, and it is unclear whether they are universally applicable to other cell types. This study is therefore aimed at understanding the specific mechanisms of action of HDIs against leukemias. We chose depsipeptide (FK228) as an HDI because it has proved to be one of the most effective HDIs against leukemias both in vitro and in vivo (Byrd et al., 1999; Murata et al., 2000; Piekarz et al., 2001; Sandor et al., 2002).

Because histone acetylation is directly linked to transcription and abnormal gene silencing is a hallmark of cancer, it is rational to carry out global gene expression profiling as an initial step to elucidate the mechanisms of action of HDIs. There are some studies dealing with this subject (Mariadason et al., 2000; Suzuki et al., 2002; Yamashita et al., 2002; Glaser et al., 2003). For example, Suzuki et al. (2002) reported that an HDI, trichostatin A, upregulated 23 genes in the colorectal cancer cell line RKO among 10,814 genes examined using a subtraction microarray. Most of them are classified as genes encoding enzymes and signal transducers, and are not growth-regulatory genes except TRADD (see below). In another study, Glaser et al. (2003) compared the gene expression profiles of three different bladder and breast cancer cell lines treated with three HDIs; SAHA, trichostatin A, and MS-27-275. They identified a common set of genes that are positively or negatively regulated by all of the HDIs in all of the cell lines tested. The common set includes 8 genes found to be upregulated and 5 genes found to be downregulated among 6,800 genes. Of the upregulated genes, p21/Cip1 seems to be most important for cell cycle arrest by HDIs. The genes encoding thymidylate synthase and CTP synthase were most prominently downregulated, which may be related to the growth arrest of these cancer cells. Because these studies were conducted with solid tumors, we adopted a similar approach in leukemic cells treated with depsipeptide (FK228), which is the most promising HDI for the treatment of leukemias. In the present study, depsipeptide (FK228) was shown to induce cell cycle arrest and apoptosis after 24 and 48 h of

TABLE 3. TNF receptor expression on FK228-treated cells

Cell line	HL-60				K562			
Incubation time	12 h		24 h		12 h		24 h	
FK228	(−)	(+)	(−)	(+)	(−)	(+)	(−)	(+)
Positivity[a]	65.5%	66.3%	66.5%	56.3%	83.1%	85.8%	86.8%	74.1%
MFI[a]	12.7	12.9	12.8	10.6	57.5	26.5	60.3	32.9

[a]Positivity and mean fluorescence intensity were determined by flow cytometry.

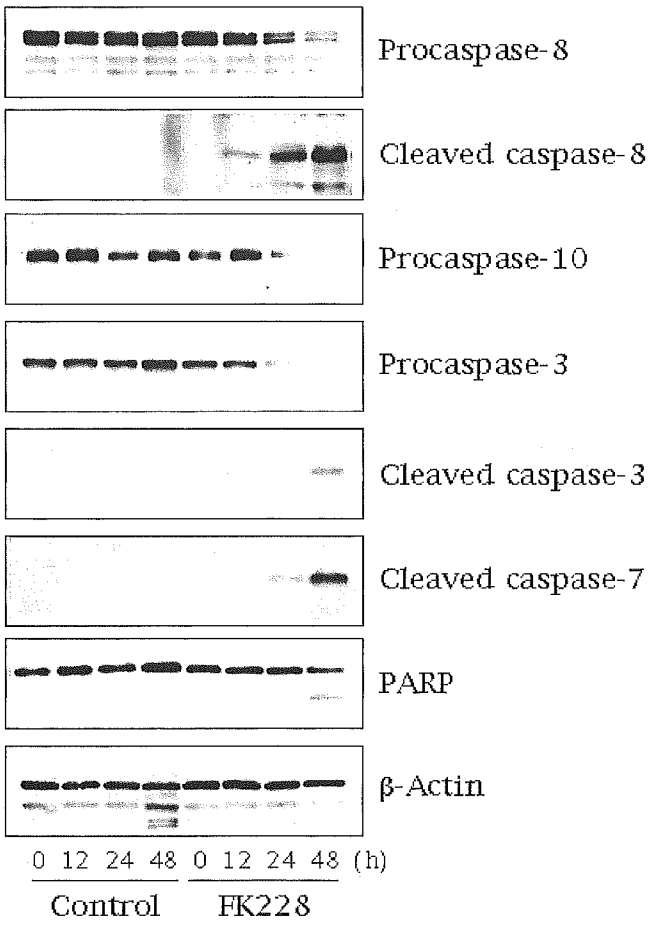

Fig. 3. Activation of the caspase cascade by depsipeptide (FK228) in HL-60 cells. HL-60 cells were cultured in the absence (control) or presence of 20 nM depsipeptide (FK228) for up to 48 h. Whole cell lysates were prepared at the indicated time points, and subjected to immunoblot analysis for procaspases-8, -10, and -3, cleaved caspases-8, -3, and -7, and PARP. The membrane filters were reprobed with anti-β-actin antibody to verify the equal loading and integrity of samples. The data shown are representative of multiple independent experiments.

culture, respectively, in HL-60 and K562 leukemic cell lines. Based on this data, we performed DNA chip analysis using RNA samples isolated at 6 h, when no apparent effect of the drug was observed. The global gene expression profiling revealed that depsipeptide (FK228) modulates a subset of genes related to growth regulation (Wee1, cdc25c, and Ki-67), checkpoint control (ATM), hematopoietic differentiation (CHED and Ikaros), cell adhesion (CD11a), signal transduction (c-fyn, NF-IL3, and A kinase anchor protein1), and apoptosis (caspases-7 and -10, DAP kinase, and FHIT) in HL-60 cells. Taking into account the time of preparing the samples, these changes are not a simple consequence of the effects of depsipeptide (FK228), but are considered to play causative roles. Our results disclose the changes in the expression of many genes that have been overlooked in similar attempts in the past, suggesting that HDIs exert cytotoxic effects via distinct mechanisms in leukemia and solid tumors.

TABLE 4. Effects of anti-TNF-α neutralizing antibody on the cytotoxicity of depsipeptide (FK228) against HL-60 cells

FK228	Additions	Proportion of cells in sub-G1 fraction (%)[a]	
−	Buffer	3.6 ± 1.2	
−	Anti-TNF-α	3.3 ± 1.2	
+	Buffer	94.1 ± 3.1	
			$P = 0.0248$*
+	Anti-TNF-α	65.8 ± 11.9	
			$P = 0.0145$**
+	Mouse IgG	94.8 ± 4.2	

[a]Means ± SD of three independent experiments.
*P-value determined by a paired Student's t-test between buffer and anti-TNF-α.
**P-value determined by a paired Student's t-test between mouse IgG and anti-TNF-α.

In addition to TNF-α, a number of TNF-related cytokines and molecules involved in TNF signaling and function were detected in DNA chip analysis. Based on this finding, we examined the involvement of the TNF/TNF receptor system in the cytotoxicity of depsipeptide (FK228), and found that autocrine TNF-α was important for the induction of apoptosis and presumably of cell cycle arrest in myeloid leukemic cell lines. The similar role of TNF-α in interferon-mediated killing of hairy cell leukemia was reported by Baker et al. (2002). Importantly, depsipeptide (FK228) enhanced the expression of caspase-10, an initiator caspase directly activated by TNF-RI-associated DISC (Wang et al., 2001), and caspase-7, an executioner caspase activated in the TNF-mediated caspase cascade (Budihardjo et al., 1999). The induction of caspases-7 and -10 may strengthen the effects of autocrine TNF-α by supplying its effector molecules in depsipeptide-treated cells. According to a recent report by Aron et al. (2003), depsipeptide activates caspase-8 through downregulation of c-FLIP, a competitive inhibitor of caspase-8, thereby inducing cell death in chronic lymphocytic leukemia cells. It is possible that the suppression of c-FLIP is another factor strengthening the effects of depsipeptide (FK228) on myeloid leukemias. Furthermore, upregulation of TRADD may also contribute to depsipeptide-induced apoptosis as an enforcer of TNF action as suggested by Suzuki et al. (Suzuki et al., 2002). An investigation is currently underway in our laboratory to test these hypotheses.

It is surprising that depsipeptide (FK228) failed to activate TNF receptor-mediated Jun kinase cascade. Downregulation of ASK1 seemed to be responsible for the failure of JNK activation (Baker and Reddy, 1998). The downregulation of ASK1 may be part of the direct inhibitory effects of depsipeptide (FK228) on Ras-MAP kinase signaling pathways (Kobayashi, Y. et al., manuscript in preparation). Our observation is indicative of selective activation by FK228 of the caspase cascade downstream of TNF receptors. A similar dissociation of the caspase cascade and JNK pathways was demonstrated in a previous study using dominant-negative FADD (Wajant et al., 1998).

We obtained evidence suggesting that autocrine TNF-α also plays a role in an accumulation of HL-60 cells in G2/M phase. This is consistent with previous reports describing TNF-α-induced G2/M arrest (Darzynkiewicz et al., 1987; Kumakura et al., 2003). However, the extent of the accumulation by TNF-α is less prominent than that in HDI-treated cells. It is therefore unlikely that HDI-induced G2 arrest is entirely due to autocrine effects of TNF-α. Additional mechanisms such as the failure of cytokinesis via hyperacetylation of the centromere may be involved in this process (Taddei et al., 2001).

Finally, we investigated the mechanisms of depsipeptide-mediated upregulation of TNF-α. We demonstrated that depsipeptide (FK228) activated transcription of the

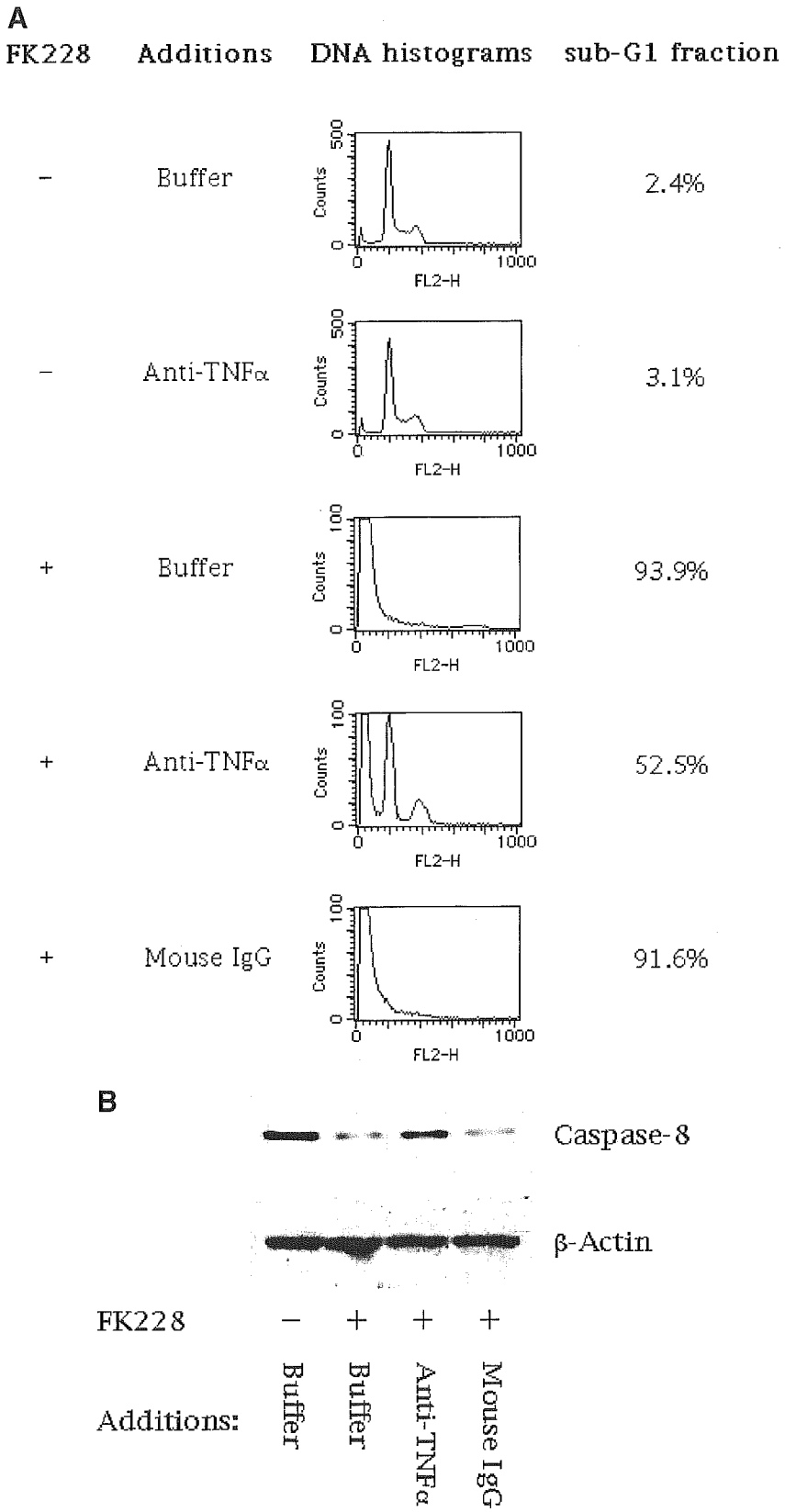

Fig. 4. Effects of a neutralizing anti-TNF-α antibody and siRNA against TNF-RI on the cytotoxicity of depsipeptide (FK228). **A**: HL-60 cells were cultured with either phosphate-buffered saline alone (buffer), purified mouse IgG (mouse IgG) or anti-TNF-α neutralizing antibody (Mab11; BD Pharmingen) (Anti-TNFα) at a final concentration of 20 μg/mL in the absence (–) or presence (+) of 20 nM depsipeptide (FK228). DNA histograms were obtained by staining cells with propidium iodide after 48 h of culture to determine the percentages of cells in sub-G1 fraction. **B**: Whole cell lysates were prepared at 48 h of culture, and subjected to immunoblot analysis for procaspases-8 and β-actin. **C**: HL-60 cells were pretreated with either siRNA against TNF-RI or its control at 50 nM for 30 h, and further cultured in the absence (–) or presence (+) of 20 nM depsipeptide (FK228). The effect of TNF-RI siRNA was confirmed by immunoblotting (left part) and flow cytometry (right upper part). DNA histograms were obtained after 48 h (right lower part). The data shown are representative of three independent experiments.